Molecular Two-Point Recognition of Fructosyl Valine and Fructosyl Glycyl Histidine in Water by Fluorescent Zn(II)-Terpyridine Complexes Bearing Boronic Acids

María K. Salomón-Flores,[a] Josue Valdes-García,[a] Alejandro O. Viviano-Posadas,[a] Diego Martínez-Otero,[b] Joaquín Barroso-Flores,[b] Iván J. Bazany-Rodríguez and Alejandro Dorazco-González*[a]

[a] Institute of Chemistry, National Autonomous University of Mexico, Ciudad Universitaria, México, 04510, CDMX, México.

[b] Centro Conjunto de Investigación en Química Sustentable, UAEM-UNAM, Carretera Toluca-Atlacomulco Km 14.5, C. P. 50200, Toluca, Estado de México, México, Instituto de Química, Universidad Nacional Autónoma de México.

[c] Facultad de Química, Universidad Nacional Autónoma de México, Ciudad Universitaria CDMX, 04510 México.

E-mail corresponding author: adg@unam.mx; orcid.org/0000-0002-7056-4237

Electronic Supporting Information

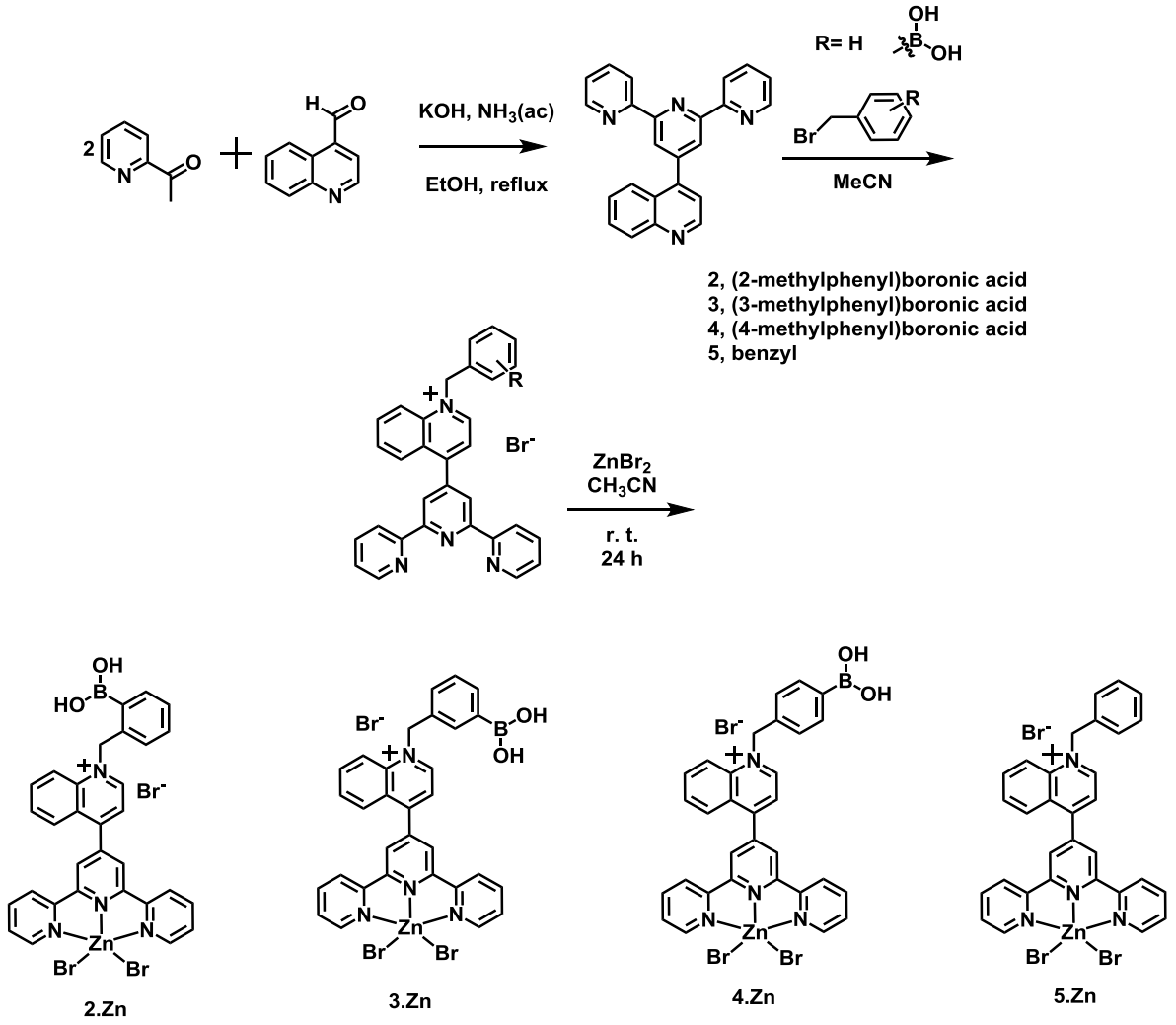

Scheme 1 General synthesis of chemosensors used in this work.

General Conditions:

Reagents and solvents were purchased as reagent grades and used without further purification.

2-acetylpiridine (Aldrich, 99%), potassium hydroxide (pellets, Tecsiquim, >85.0%), 4-quinolinecarboxaldehyde (Aldrich, 97), 3-(bromomethyl)phenylboronic acid (Aldrich, 90%), ethanol (Tecqsiquim, >99.5%), acetonitrile (Tecsiquim, 99.5%), ammonium hydroxide solution (Aldrich, 29.50%), 2-(bromomethyl)phenylboronic acid (Aldrich, 90%), 4-(bromomethyl)phenylboronic acid (Aldrich, 90%), ethyl acetate (Aldrich, >99.5%), ethyl ether (Tecquisim, >99%), benzyl bromide (Aldrich, 98%), zinc bromide dihydrate (Aldrich, 99%), D-(+)-glucose (Aldrich, >99.5%), L-valine (Aldrich, >98%), glacial acetic acid (Tecquisim, 99.7%), pyridine (Aldrich, >99%), glycyl L-histidine (Aldrich, >99%), CD_3OD (Aldrich, >99%), dimethyl sulfoxide-d_6 (Aldrich, 99.5%), 3-(N-Morpholino)propanesulfonic acid, MOPS (Aldrich, 99.5%), sodium hydroxide (Tecsiquim, 97 %), deionized water. MOPS buffer solution (10 mM, pH 7.4) was prepared with deionized water. Stock solutions of fructosyl amino acids, monosaccharides and amino acids 50 mM were prepared in deionized water. A stock solutions of corresponding Zn(II)-complex 1.0 mM, were made with acetonitrile.

Fluorescence and UV-Vis spectra were recorded on an Agilent Cary Eclipse fluorimeter and an Agilent Cary 100 spectrophotometer, respectively, both equipped with a thermostated cell holder at 25°C (±0.1). The source for Cary Eclipse was a 75W Xenon short arc lamp.

Fluorescence lifetime measurements: A Time Correlated Single Photon Counting (TCSPC) system coupled to a custom-built confocal microscope was used to acquire the fluorescence lifetimes. A 354 nm picosecond laser pulsed at 10 MHz (LDH-DC-405, PicoQuant) was focused into a 1 cm quartz cell with a 0.85 NA microscope objective. The fluorescence collected with the same objective passed through a 366 nm long-pass dichroic mirror (Chroma T510lpxrxt), a 364 nm notch filter (Chroma ZET405nf), and a 425 nm long pass emission filter (Chroma ET425lp) and was focused to an avalanche photodiode (PD-050-CTE, MPD). The laser controller (PDL-800-D, PicoQuant) and the APD were connected to a TCSPC card (PicoHarp 300, PicoQuant). The power of irradiation was controlled to obtain less than 1% of the detection events in order to avoid pile-up effects on the recorded histogram. Allura Red (analytical standard Sigma-Aldrich) was used to obtain the IRF under the same conditions of irradiation. All data were obtained and treated in SymphoTime 64 software (PicoQuant).

^{1}H and ^{13}C NMR spectra were recorded on a Bruker Advance DPX 400 spectrometer at 400, 100 MHz respectively. ^{11}B NMR spectra were recorded on a Bruker Advance at 96 MHz and are reported in parts per million with respect to BF_3OEt_2 (δ=0).

High-Resolution Electrospray Ionization mass with positive scan spectra for FGH and **3Zn** were obtained with a Bruker Micro TOF II. Electrospray Ionization mass spectrum with positive and negative scan for all synthesized molecules were obtained with a Waters CapLCcoupled Micromass Q-ToF Ultima ESI-instrument.

Table S1. Crystallographic data and structure refinement for **3Zn** and **5Zn**

Crystal data	**3Zn**	**5Zn**
Empirical formula	$C_{33}H_{34}BBr_3N_4O_5Zn$	$C_{99}H_{82.68}Br_{11}N_{14.77}O_{2.23}Zn_4$
Formula weight (g mol^{-})	882.55	2655.41
Temperature (K)	100(2)	100(2)
Wavelength	0.71073 Å	0.71073
Crystal system	Monoclinic	Triclinic
Space group	$P2_1/c$	P-1
a (Å)	8.3543(3)	11.9341(7)
b (Å)	15.2716(6)	13.9809(8)
c (Å)	27.3324(10)	29.8353(17)
α (°)	90	87.8007(11)
β (°).	92.6004(8)	84.5345(11)
γ = 90°.	90	88.1333(12)
Volume (Å)	3483.6(2)	4949.6(5)
Z	4	2
Density calculated (mg/m^3)	1.683	1.782
Absorption coefficient (mm^{-1})	4.192	5.455
F(000)	1760	2606
Crystal size (mm^3)	0.429 x 0.215 x 0.200	0.187 x 0.140 x 0.100
Theta range for data collection (°)	2.001 to 27.445	1.786 to 27.485
Index ranges	-10<=h<=10, -19<=k<=19, -35<=l<=35	-15<=h<=15, -18<=k<=18, -38<=l<=38
Reflections collected	39910	91894
Independent reflections	7964 [R(int) = 0.0375]	22705[R(int) = 0.0461]
Completeness to theta = 25.242°	100.0 %	99.9 %
Refinement method	Full-matrix least-squares on F^2	Full-matrix least-squares on F^2
Data / restraints / parameters	7964 / 95 / 478	22705 / 3001 / 1689
Goodness-of-fit on F^2	1.032	1.055
Final R indices [I>2sigma(I)]	R1 = 0.0272, wR2 = 0.0673	R1 = 0.0404, wR2 = 0.0887
R indices (all data)	R1 = 0.0333, wR2 = 0.0697	R1 = 0.0574, wR2 = 0.0946
Extinction coefficient	n/a	n/a
Largest diff. peak and hole ($e.Å^{-3}$)	0.840 and -0.638	1.492 and -1.448

Table S2. Hydrogen Bonds for **3Zn** [Å and °].

D-H...A	d(D-H)	d(H...A)	d(D...A)	<(DHA)
O(1)-H(1)...O(5)	0.852(10)	1.897(18)	2.697(3)	156(3)
O(2)-H(2A)...Br(3^a)	0.846(10)	2.392(11)	3.2348(19)	173(3)
O(4)-H(4A)...Br(2)#1	0.846(10)	2.542(12)	3.378(2)	170(3)
O(4)-H(4B)...O(3^a)	0.850(10)	1.908(12)	2.756(6)	175(4)
O(4)-H(4B)...O(3A^b)	0.850(10)	1.92(3)	2.77(3)	175(4)
O(5)-H(5A)...O(4)	0.862(10)	1.948(18)	2.773(3)	160(4)
O(5)-H(5B)...Br(3^a)#2	0.853(10)	2.468(11)	3.319(2)	176(4)
O(3^a)-H(3^a)...Br(3^a)	0.84	2.65	3.404(6)	150.6

Symmetry transformations used to generate equivalent atoms:

#1 -x+1,-y+1,-z+1 #2 -x+2,y-1/2,-z+1/2

Table S3. Hydrogen Bonds for **5Zn** [Å and °]

D-H...A	d(D-H)	d(H...A)	d(D...A)	<(DHA)
O(1)-H(1OA)...Br(7)#1	0.841(10)	2.494(12)	3.328(3)	172(5)
O(1)-H(1OB)...Br(7)	0.843(10)	2.491(13)	3.327(3)	172(4)
O(2)-H(2OA)...Br(8^a)	0.847(10)	2.84(6)	3.407(9)	126(6)
O(2)-H(2OA)...Br(8A^b)	0.847(10)	2.76(6)	3.311(12)	124(6)
O(2)-H(2OA)...N(15A^b)	0.847(10)	2.22(6)	2.799(7)	126(7)
O(2)-H(2OA)...N(15C^c)	0.847(10)	2.68(6)	3.151(4)	116(5)

Symmetry transformations used to generate equivalent atoms:

#1 -x+2,-y+1,-z+1

Table S4. Selected bond distances (Å) and angles (°) for boron atom in crystal **3Zn**

3Zn	
O(1)-B(1)	1.352(4)
O(2)-B1	1.353(3)
C(28)-B(1)	1.574(4)
O(1)-B(1)-O(2)	120.1(3)
O(1)-B(1)-C(28)	123.5(2)
O(2)-B(1)-C(28)	116.4(2)

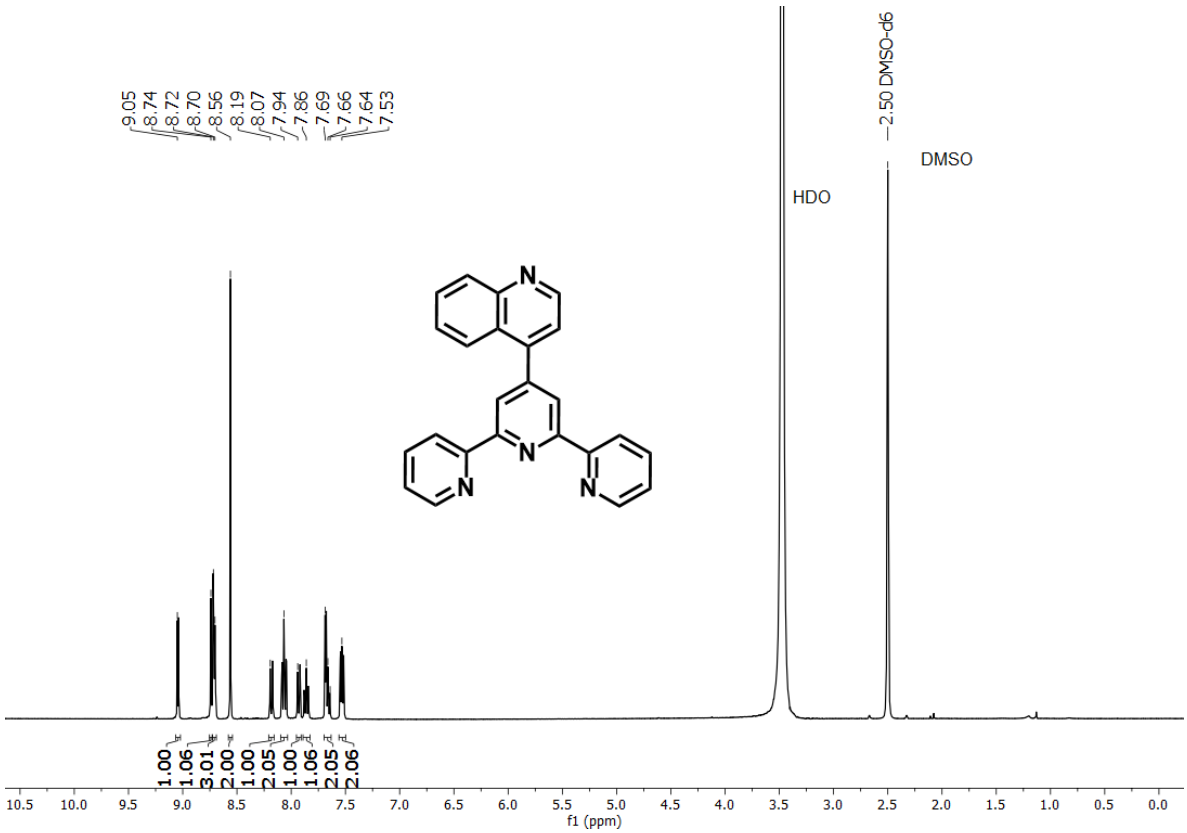

Fig. S1. [1]H NMR (300 MHz, 25°C) spectrum of **1** in DMSO-d_6.

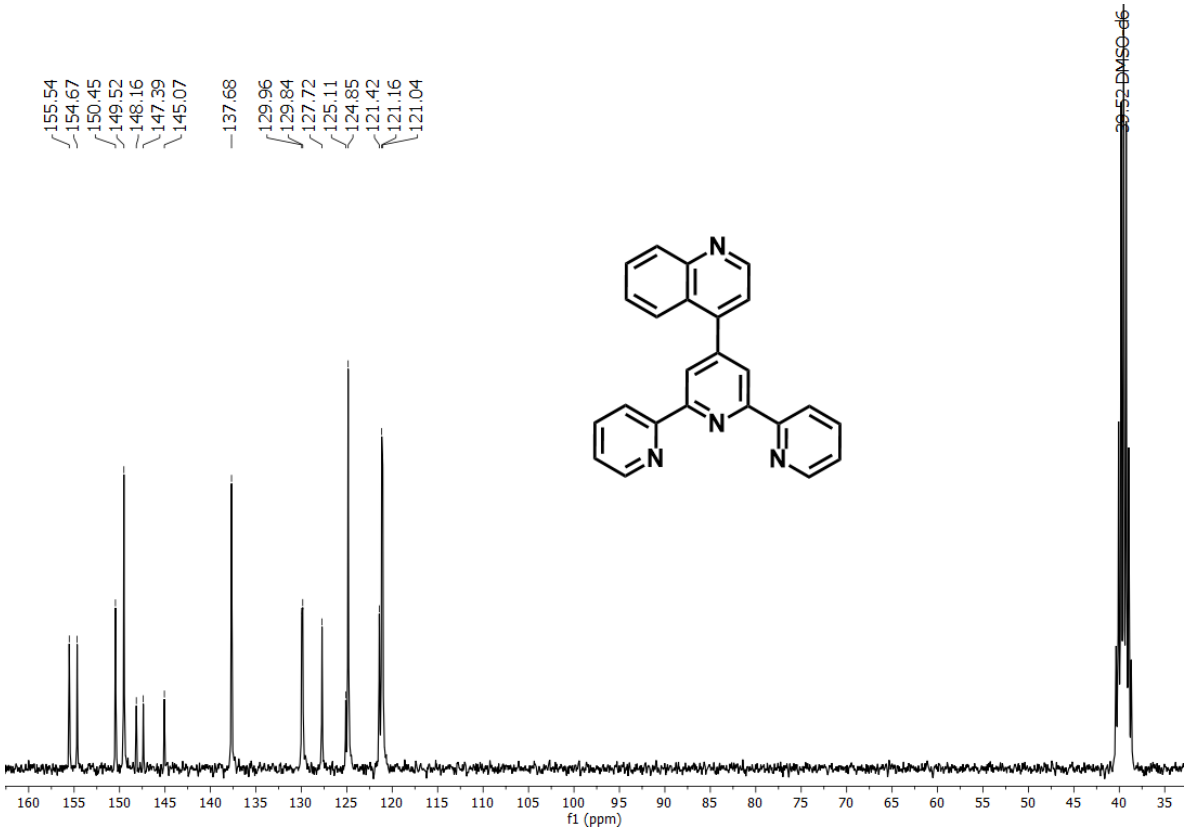

Fig. S2. [13]C NMR (75 MHz, 25°C) spectrum of **1** in DMSO-d_6

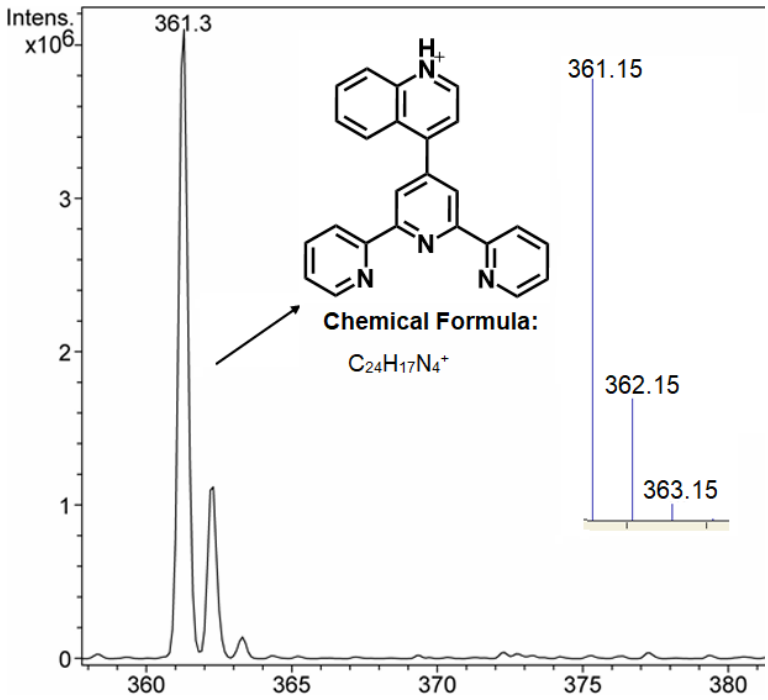

Fig. S3. Positive scan MS-ESI spectrum of **1**. Inset: theoretically calculated MS isotopic patterns.

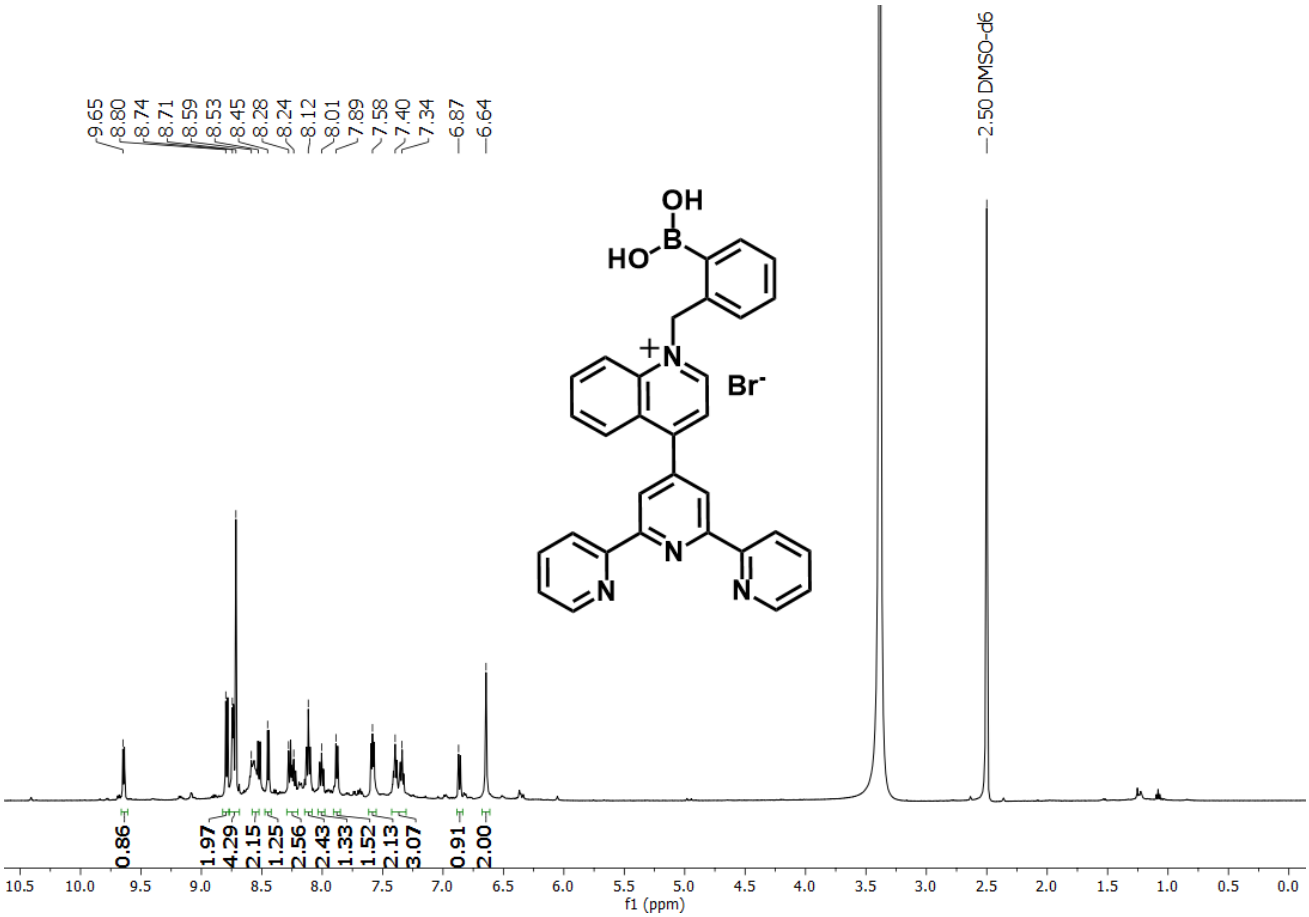

Fig. S4. ^{1}H NMR (300 MHz, 25°C) spectrum of **2** in DMSO-d_6.

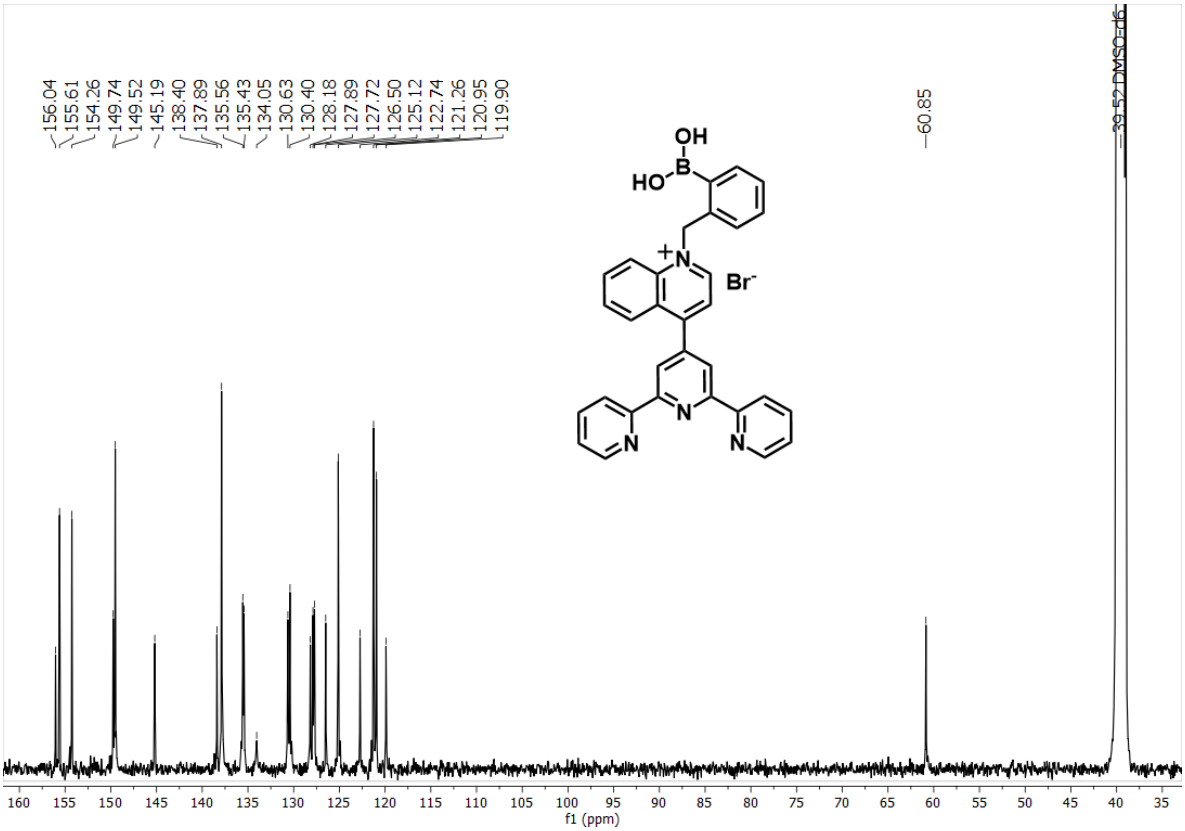

Fig. S5. ^{13}C NMR (75 MHz, 25°C) spectrum of **2** in DMSO-d_6.

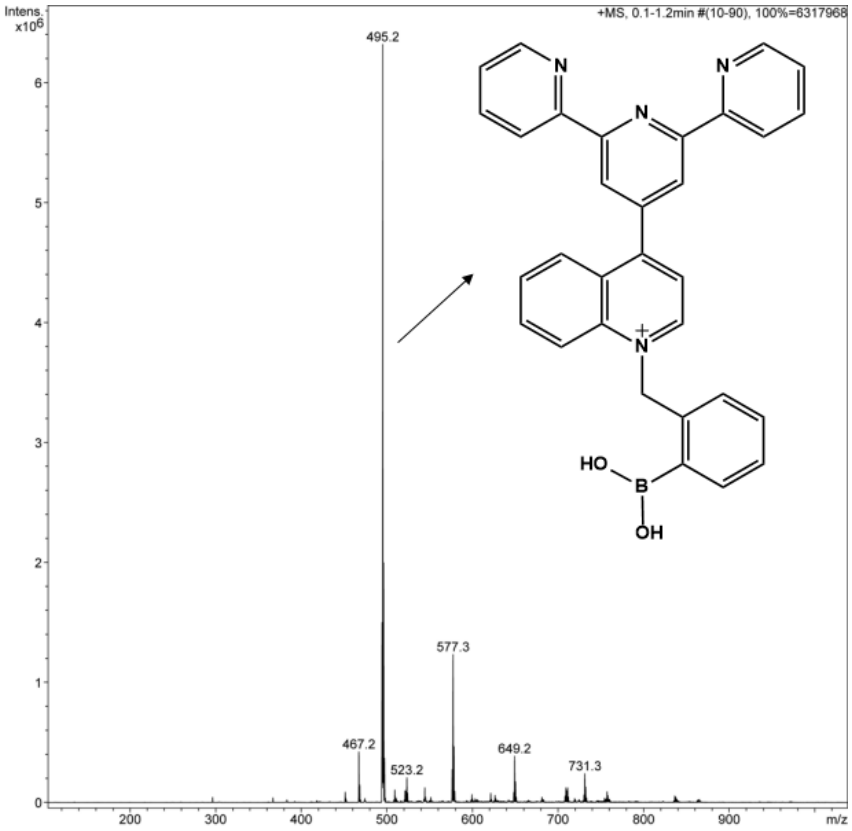

Fig. S6. Positive scan MS-ESI spectrum of **2**.

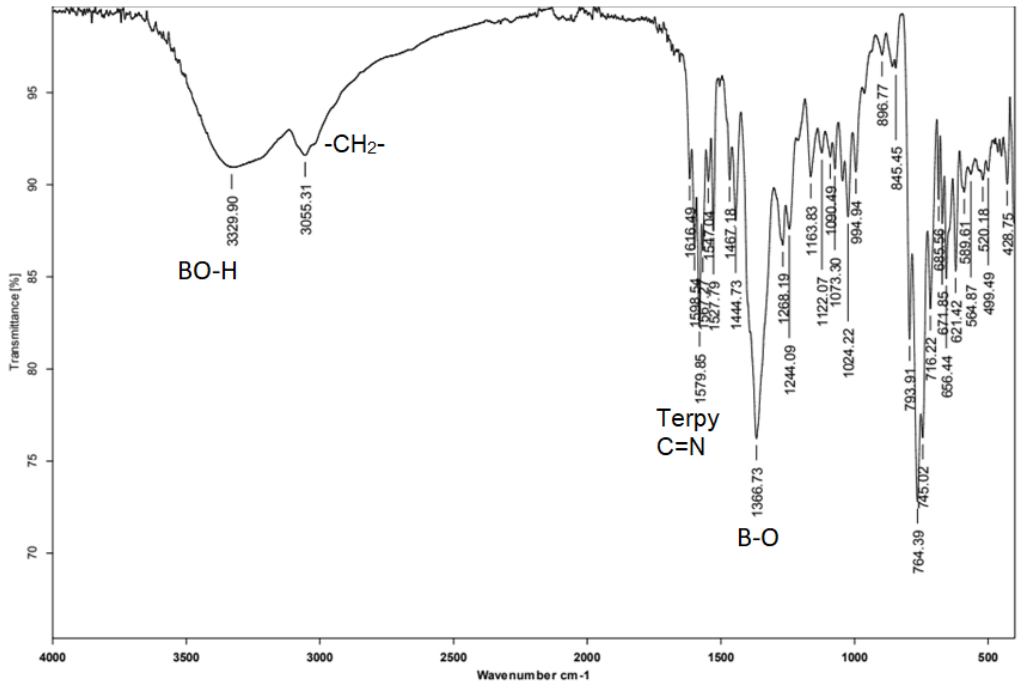

Fig. S7. IR (ATR) spectrum of **2**.

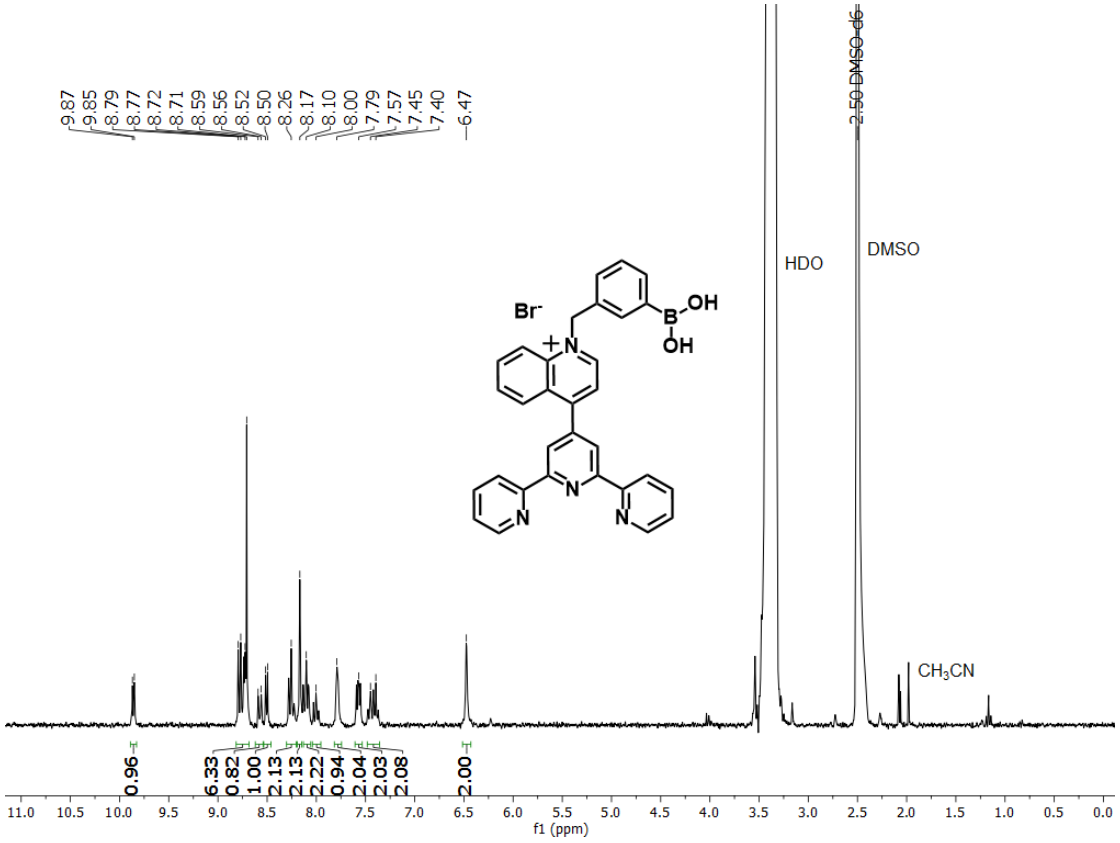

Fig. S8. ^{1}H NMR (300 MHz, 25°C) spectrum of **3** in DMSO-d_6.

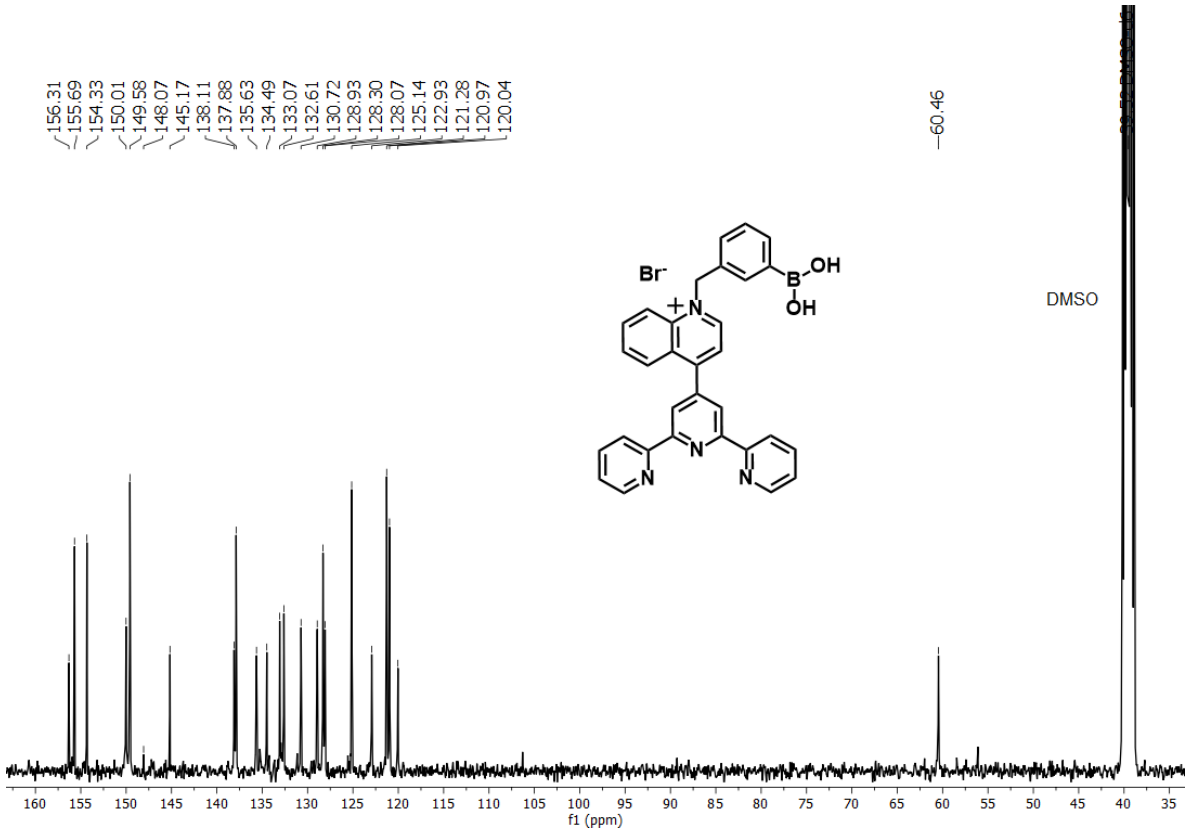

Fig. S9. ^{13}C NMR (75 MHz, 25 °C) spectrum of **3** in DMSO-d_6.

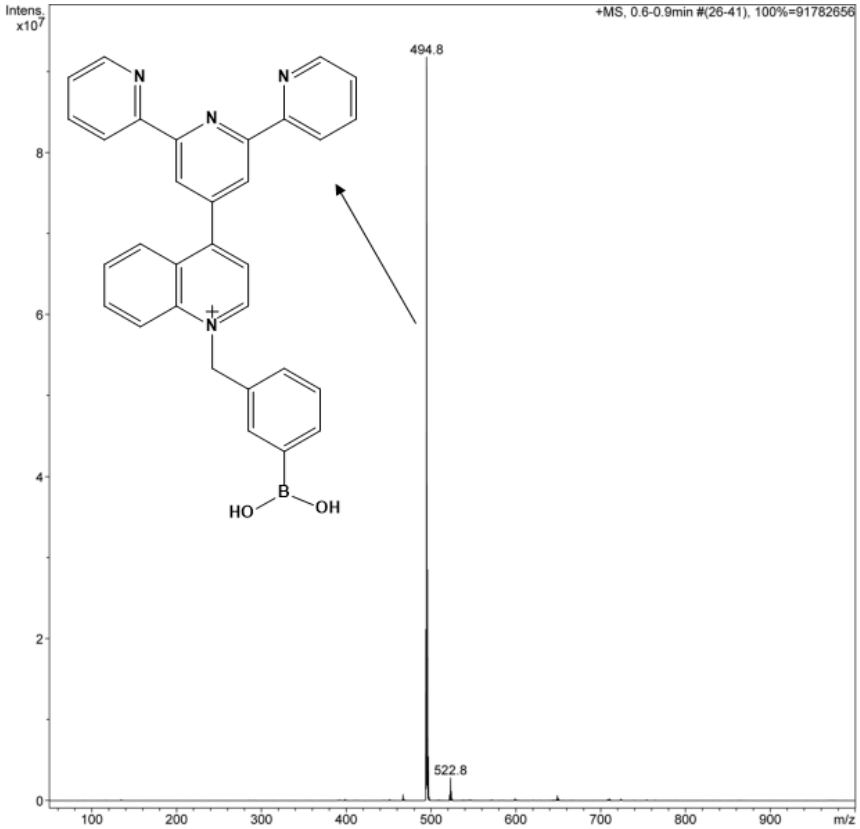

Fig. S10. Positive scan MS-ESI spectrum of **3**.

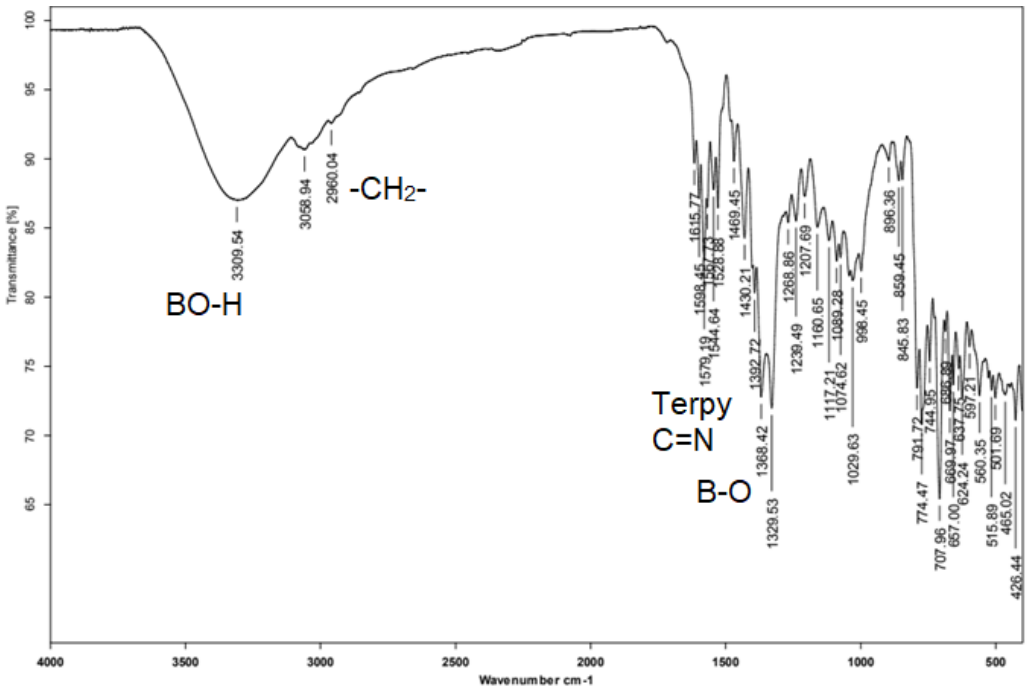

Fig. S11. IR (ATR) spectrum of **3**.

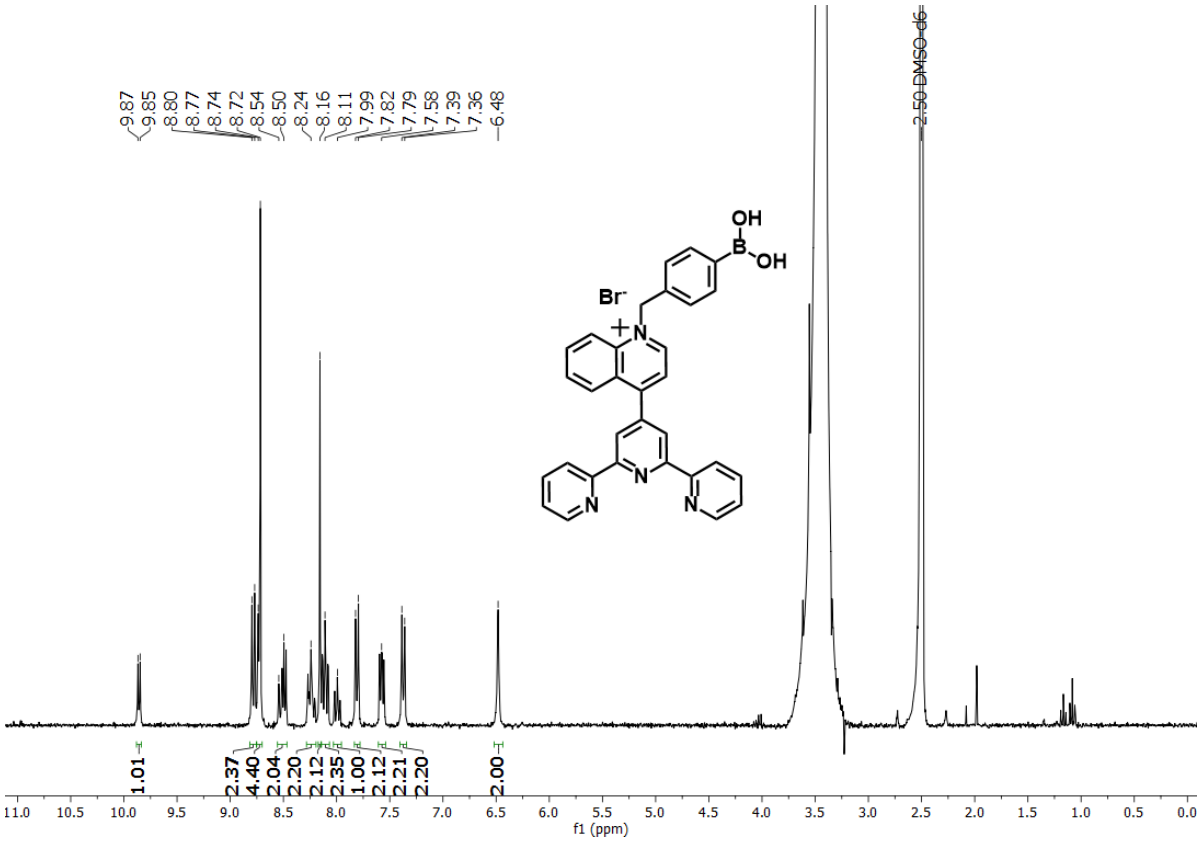

Fig. S12. ^{1}H NMR (300 MHz, 25°C) spectrum of **4** in DMSO-d_6.

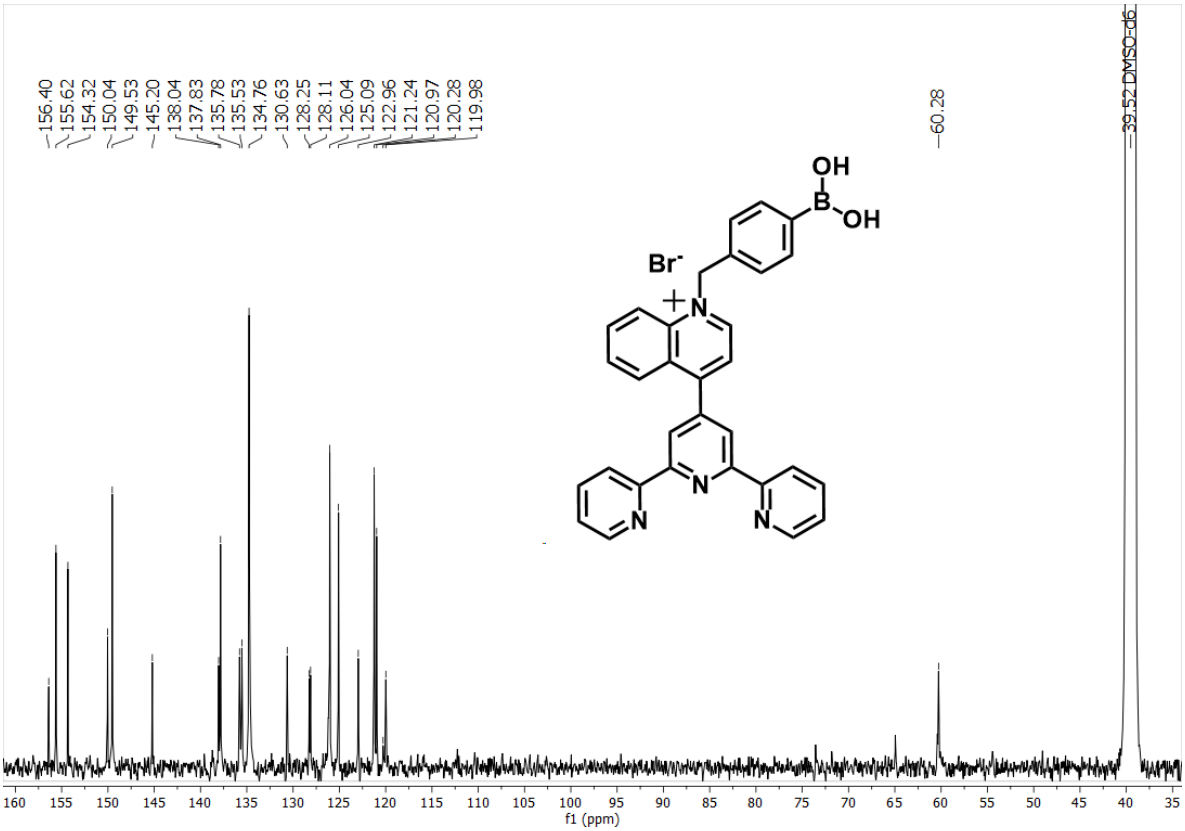

Fig. S13. ^{13}C NMR (75 MHz, 25°C) spectrum of **4** in DMSO-d_6.

Fig. S14. Positive scan MS-ESI spectrum of **4**.

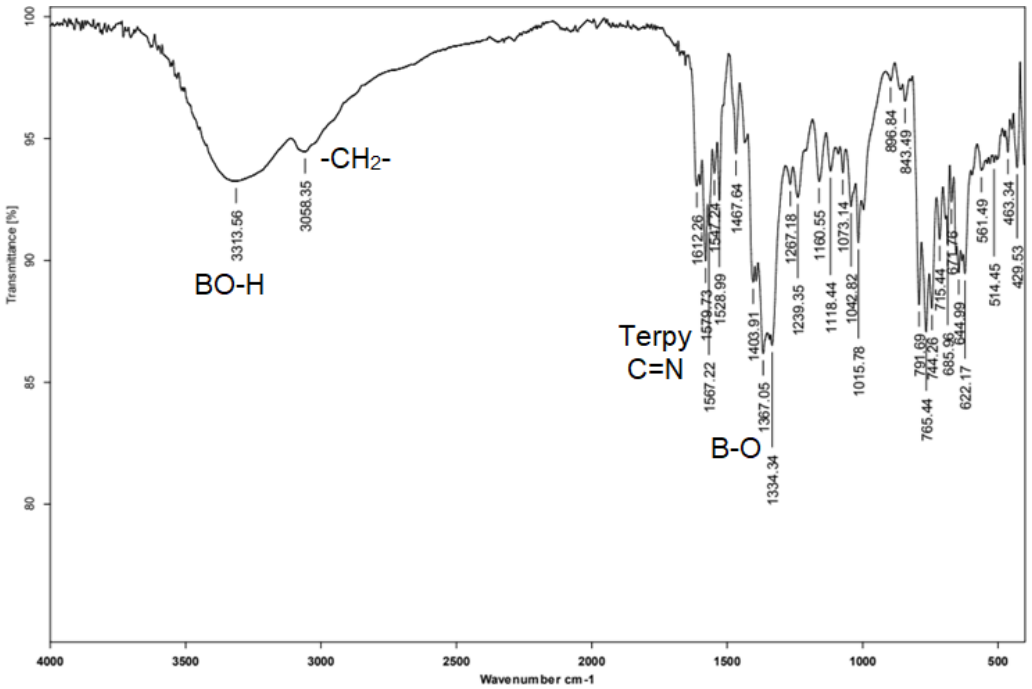

Fig. S15. IR (ATR) spectrum of **4**.

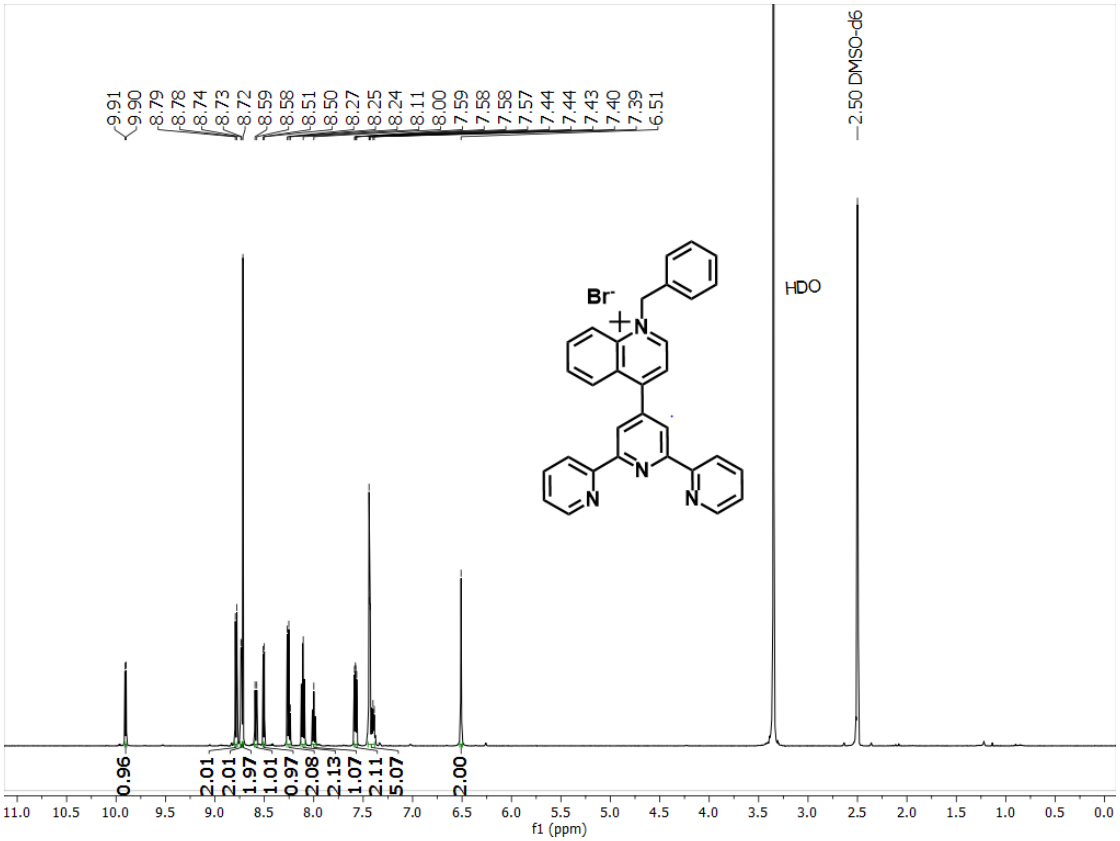

Fig. S16. ^{1}H NMR (300 MHz, 25°C) spectrum of **5** in DMSO-d_6.

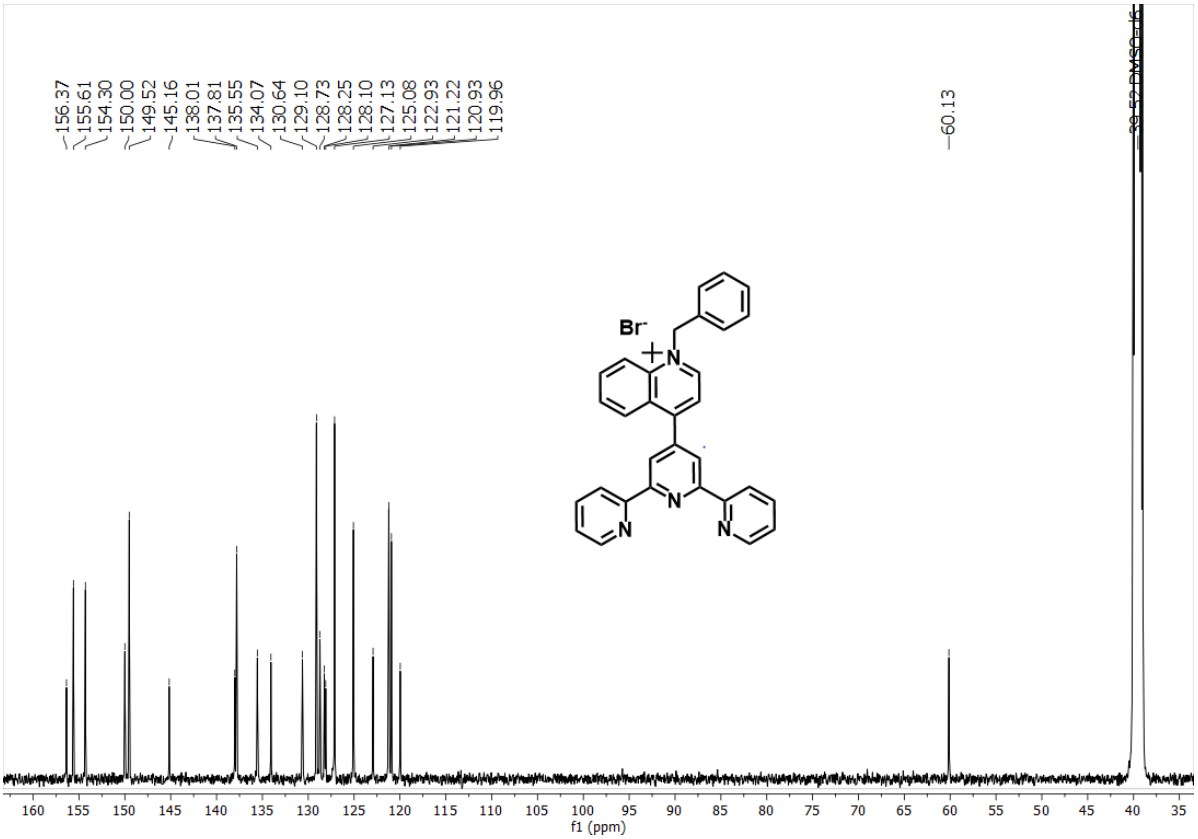

Fig. S17. ^{13}C NMR (75 MHz, 25°C) spectrum of **5** in DMSO-d_6.

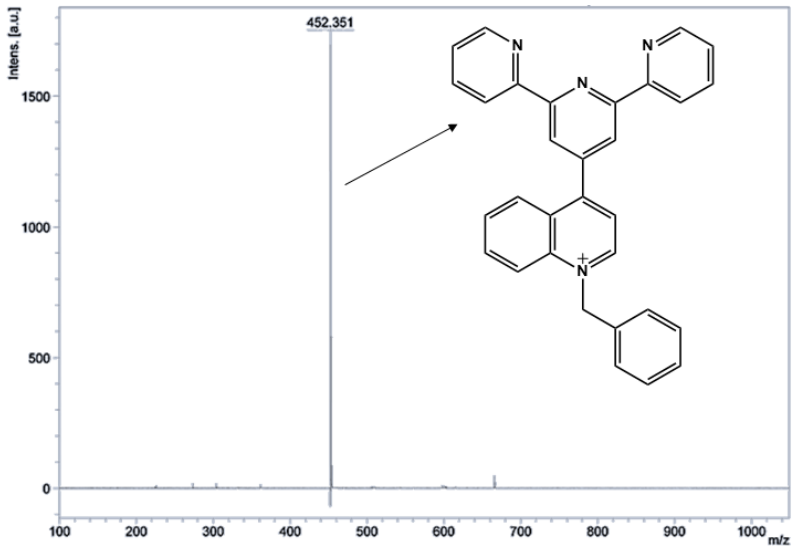

Fig. S18. Positive scan MALDI-TOF spectrum of **5**.

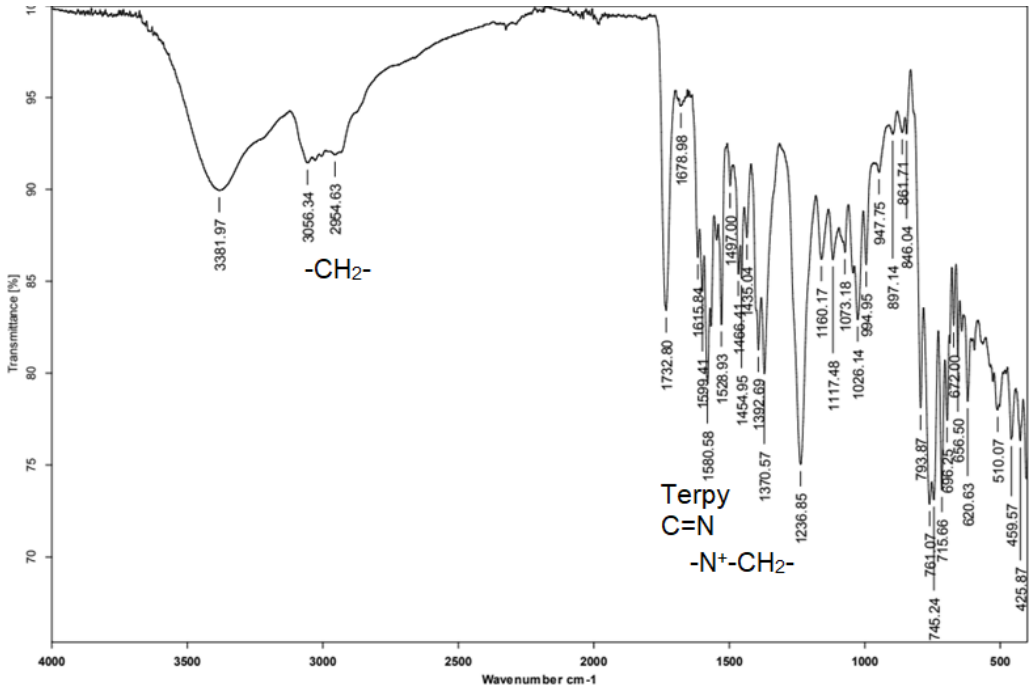

Fig. S19. IR (ATR) spectrum of **5**.

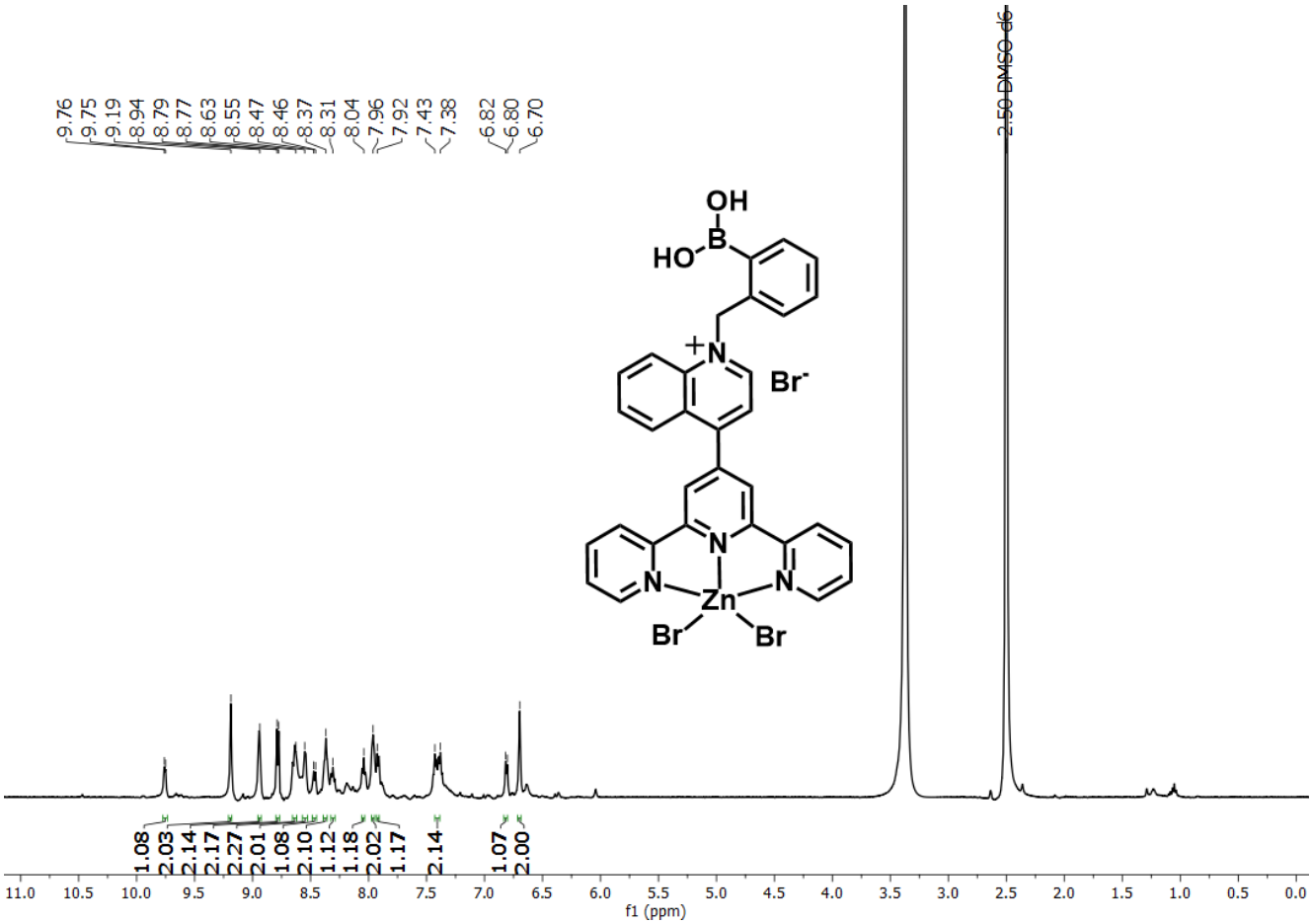

Fig. S20. ^{1}H NMR (300 MHz, 25°C) spectrum of **2Zn** in DMSO-d_6.

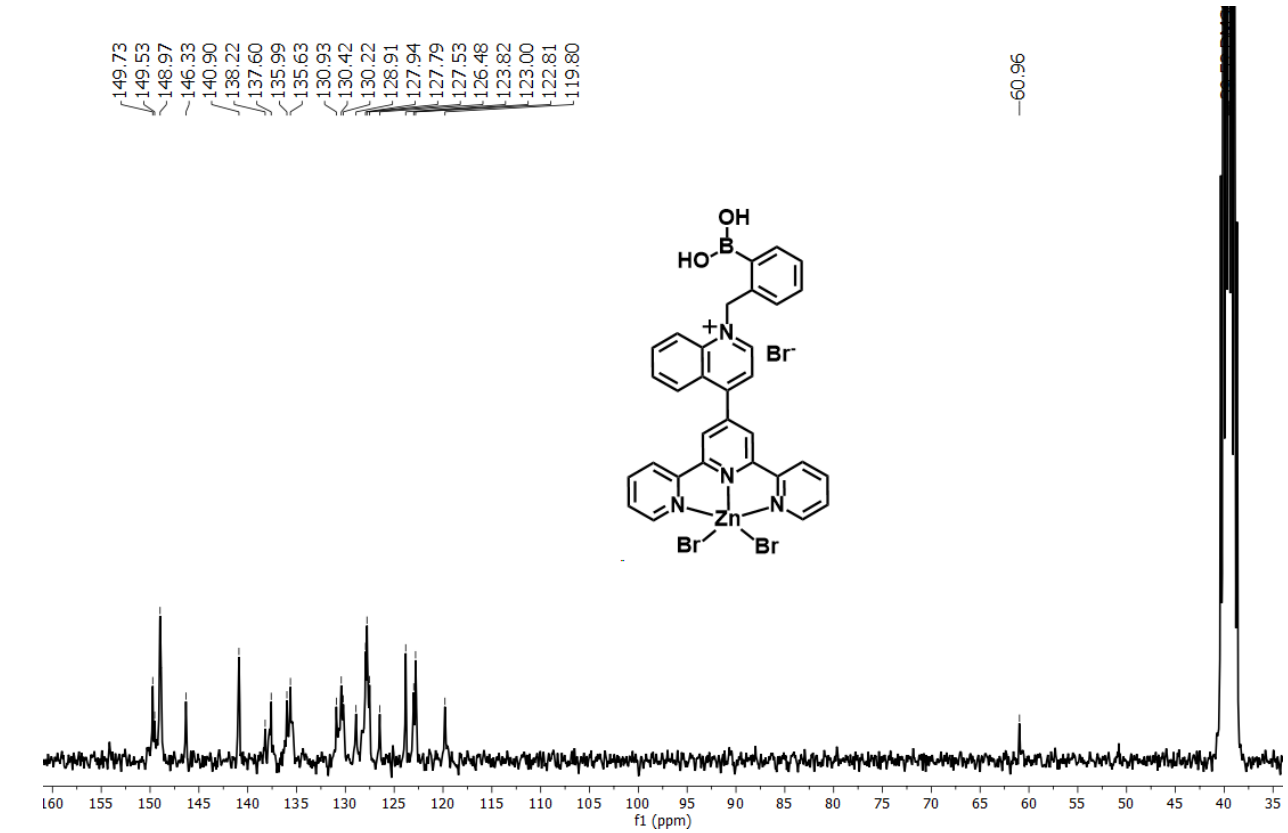

Fig. S21. ^{13}C NMR (75 MHz, 25°C) spectrum of **2Zn** in DMSO-d_6.

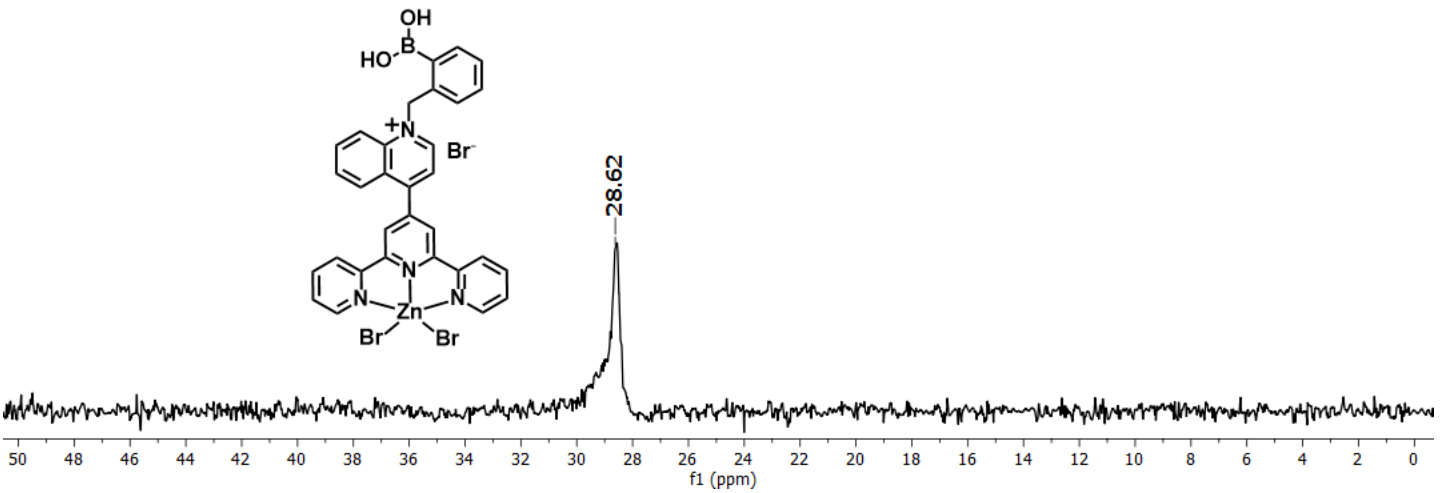

Fig. S22. ^{11}B NMR (96 MHz, 25 °C) spectrum of **2Zn** in MeOD-DMSO-d_6 (v/v, 4/1).

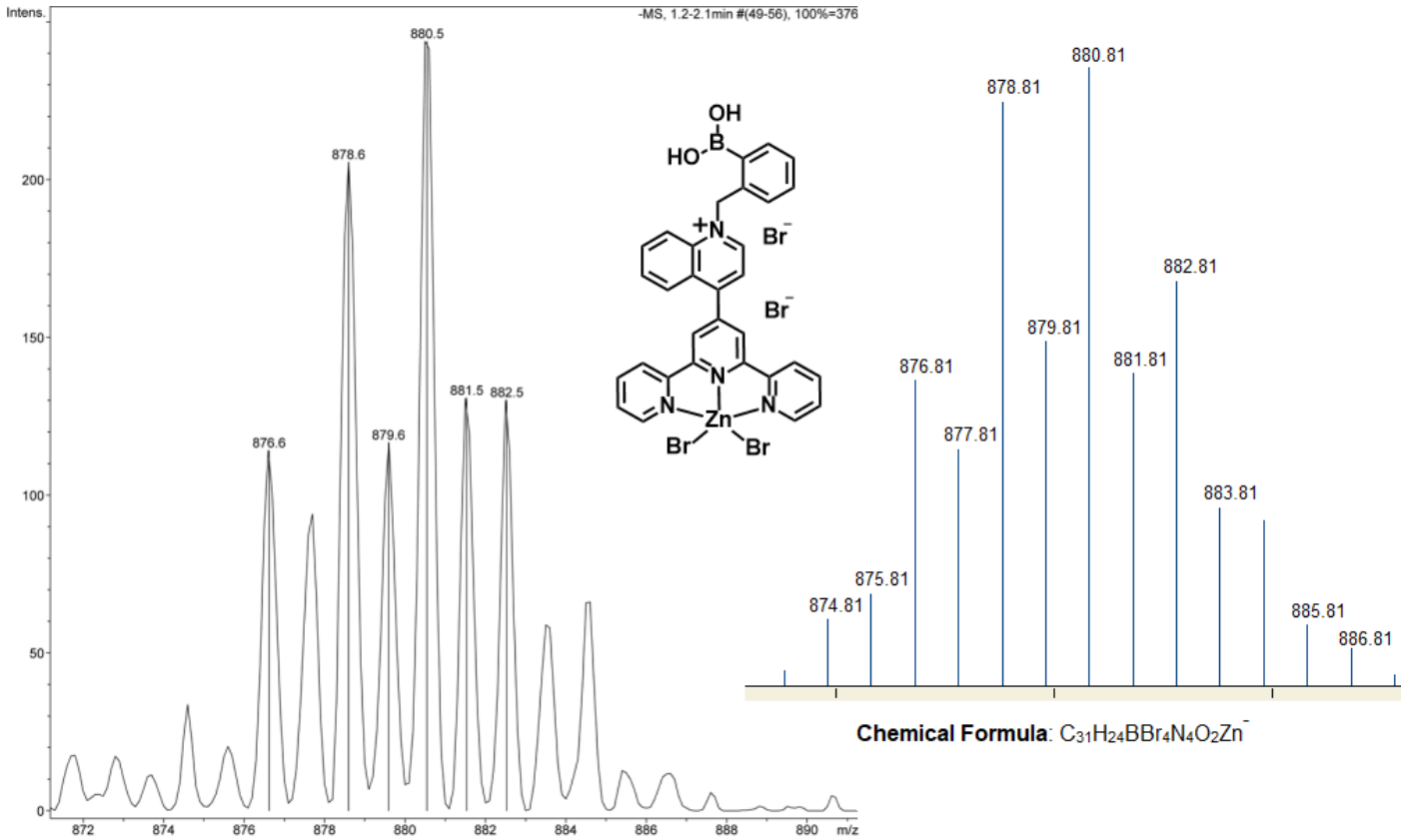

Fig. S23. Negative scan MS-ESI spectrum of **2Zn**. Inset: theoretically calculated MS isotopic patterns.

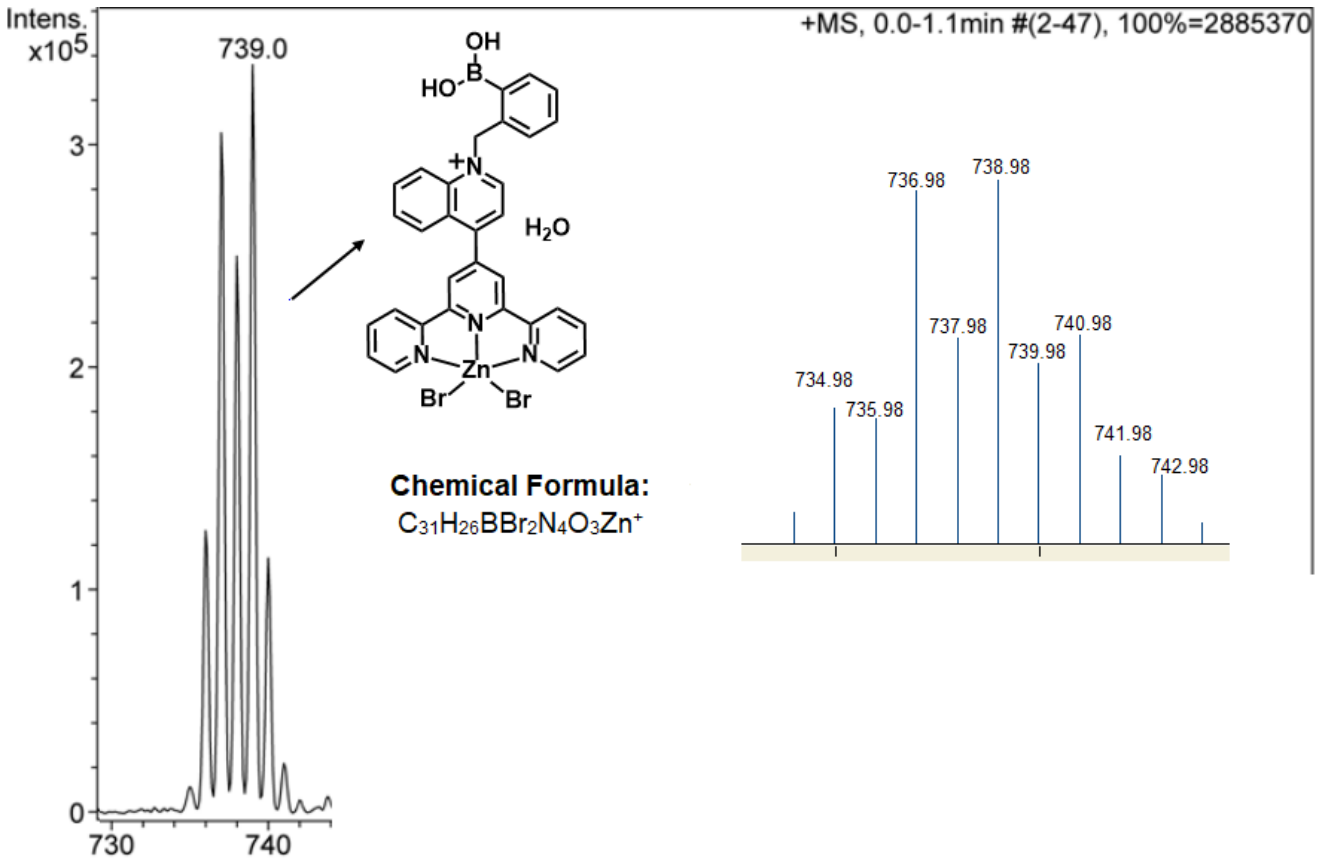

Fig. S24. Positive scan MS-ESI spectrum of **2Zn**. Inset: theoretically calculated MS isotopic patterns.

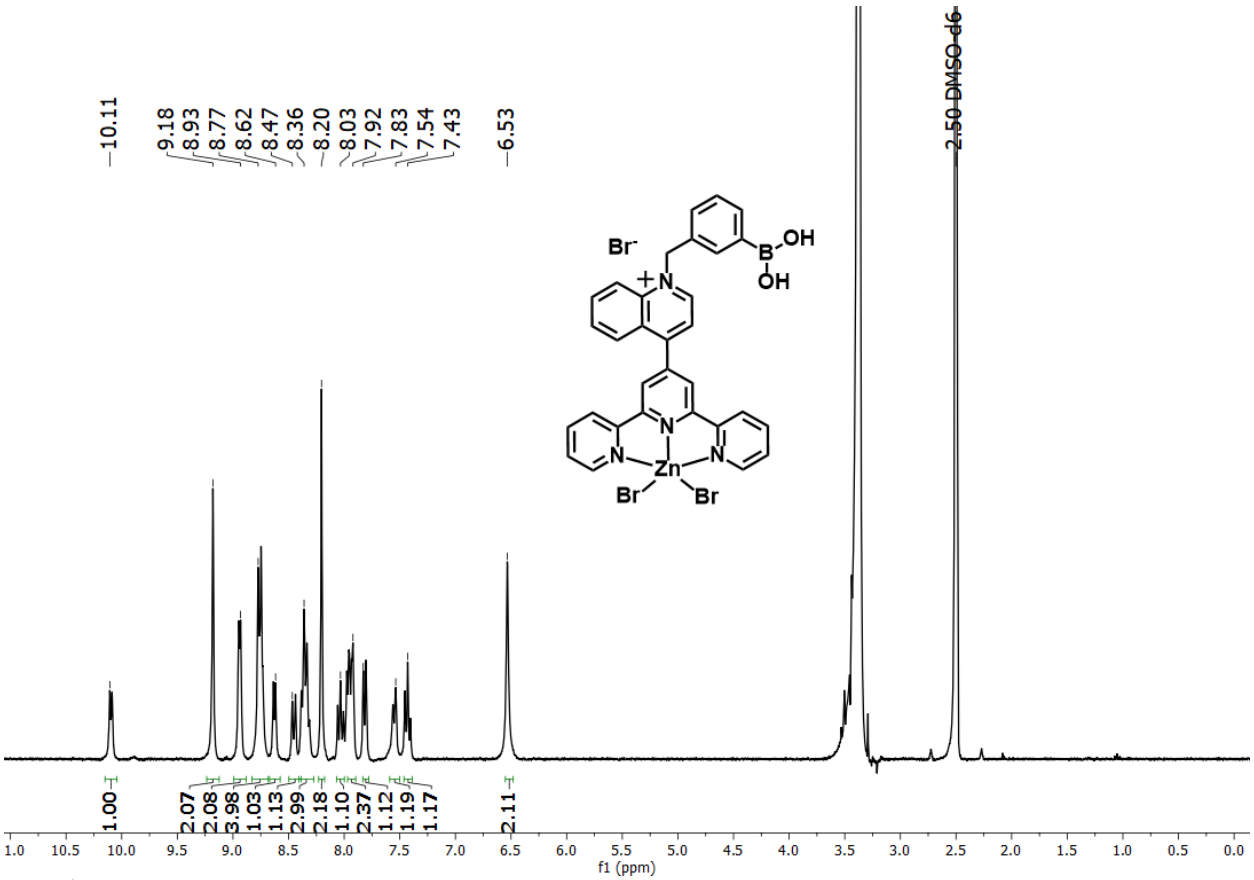

Fig. S25. ^{1}H NMR (300 MHz, 25°C) spectrum of **3Zn** in DMSO-d_6.

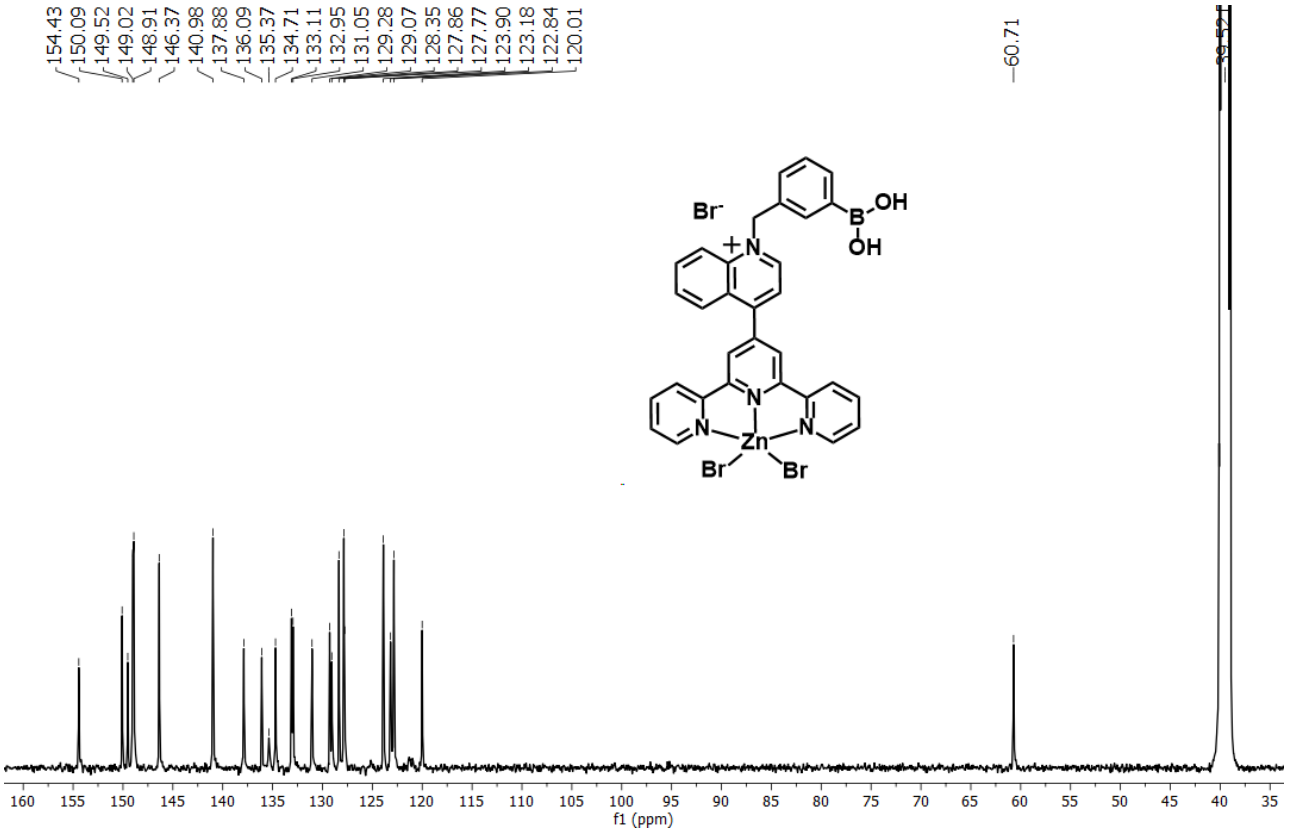

Fig. S26. ^{13}C NMR (75 MHz, 25°C) spectrum of **3Zn** in DMSO-d_6.

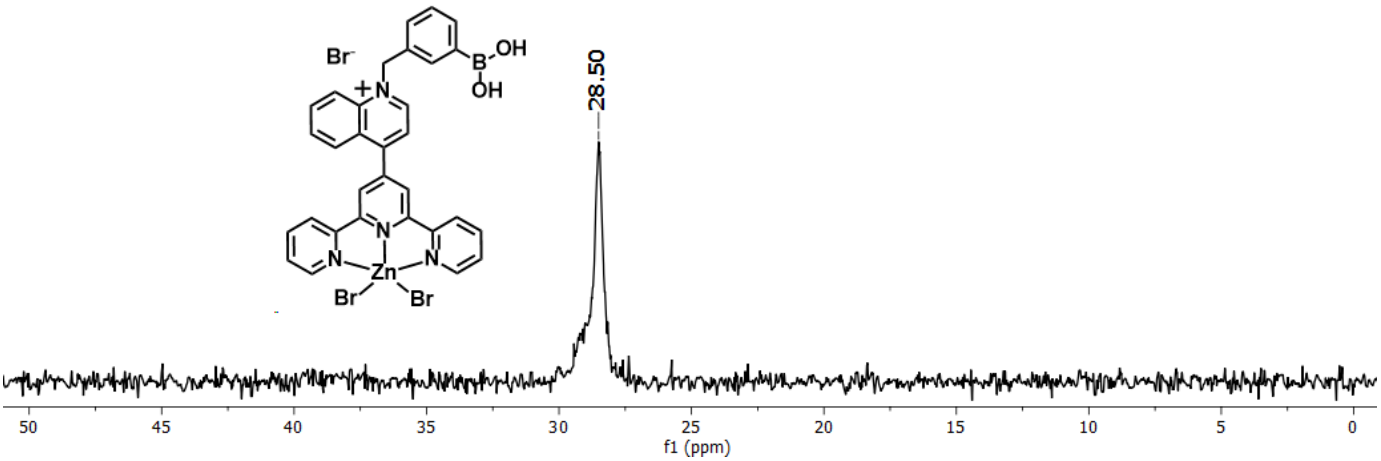

Fig. S27. ^{11}B NMR (96 MHz, 25 °C) spectrum of **3Zn** in MeOD-DMSO-d_6 (v/v, 4/1).

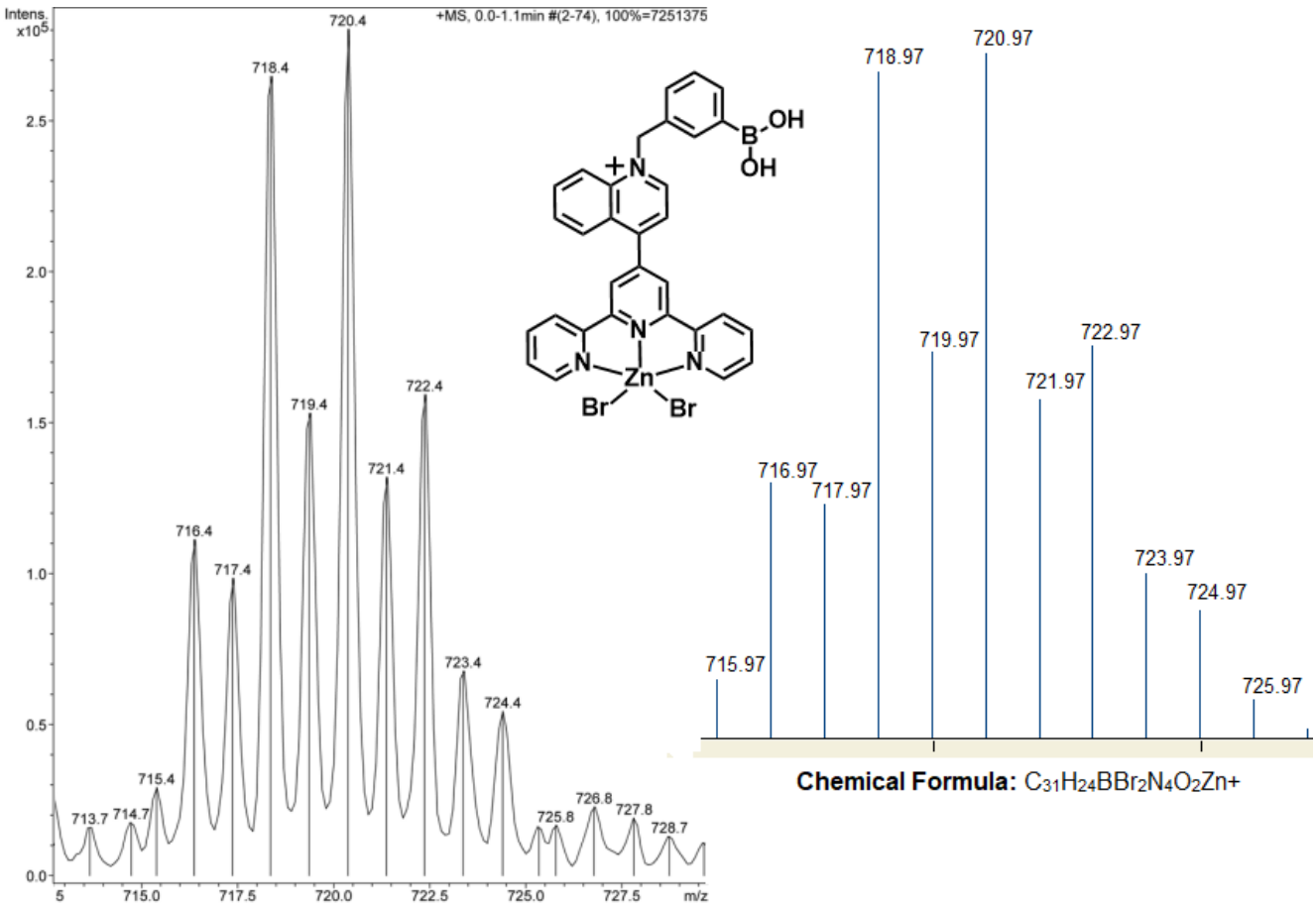

Fig. S28. Positive scan MS-ESI spectrum of **3Zn**. Inset: theoretically calculated MS isotopic patterns.

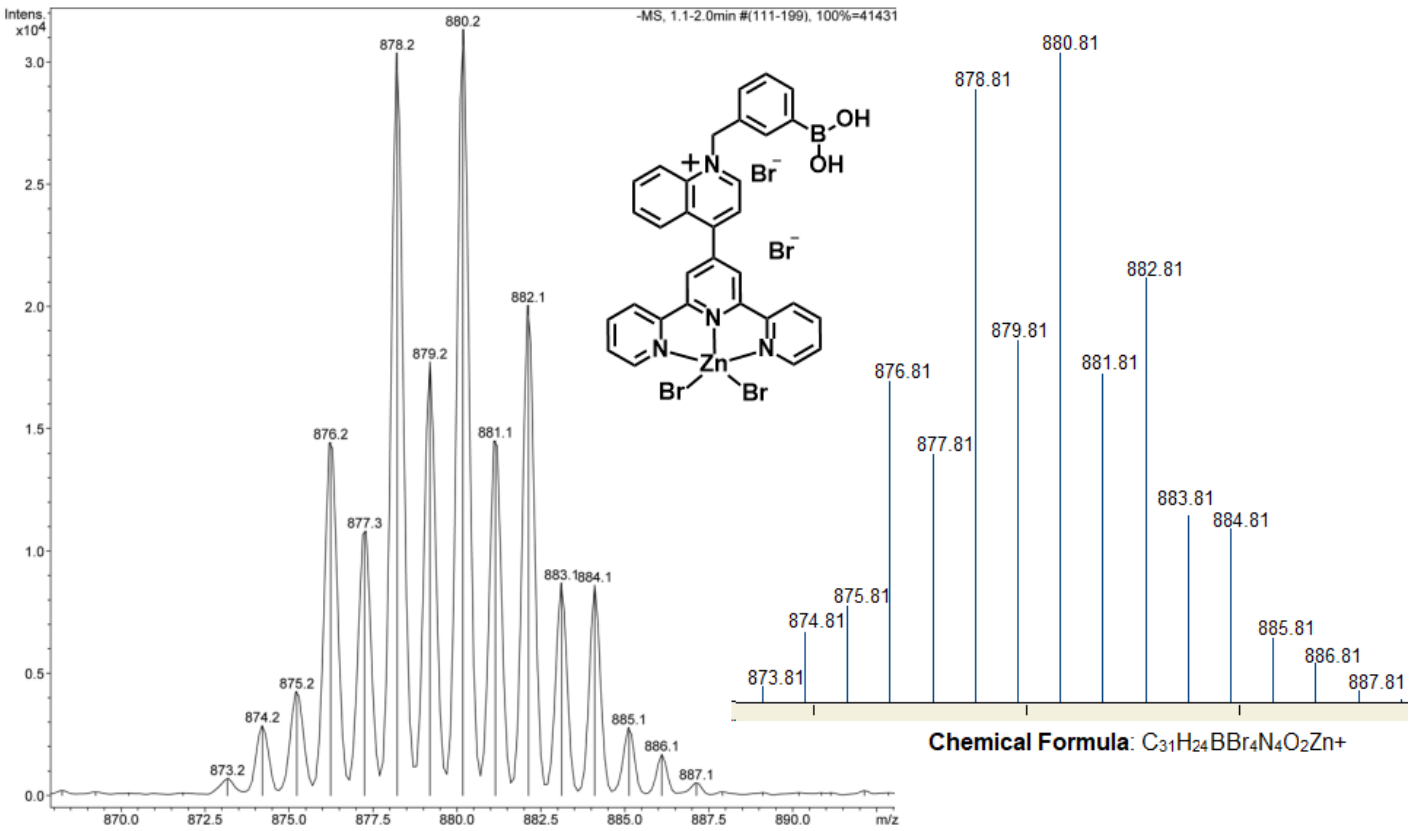

Fig. S29. Negative scan MS-ESI spectrum of **3Zn**. Inset: theoretically calculated MS isotopic patterns.

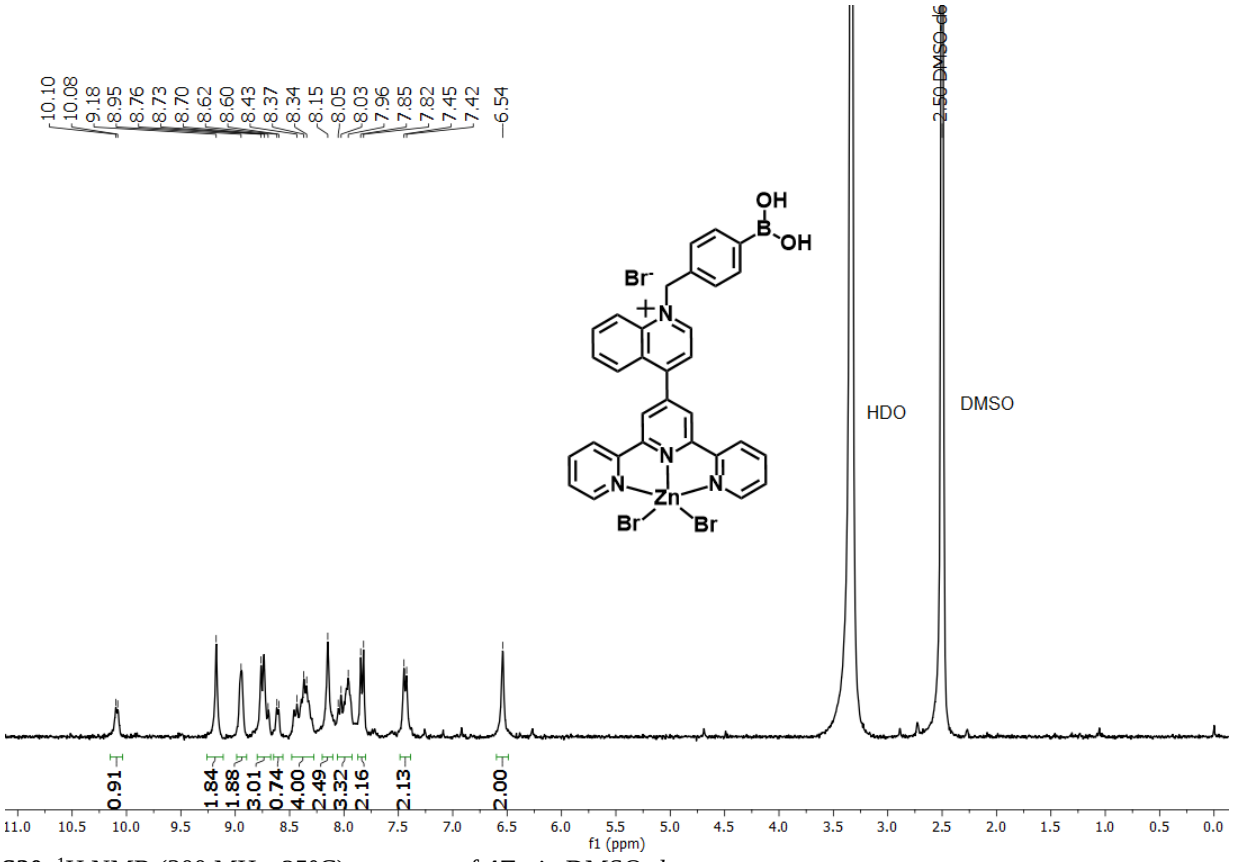

Fig. S30. ^{1}H NMR (300 MHz, 25°C) spectrum of **4Zn** in DMSO-d_6.

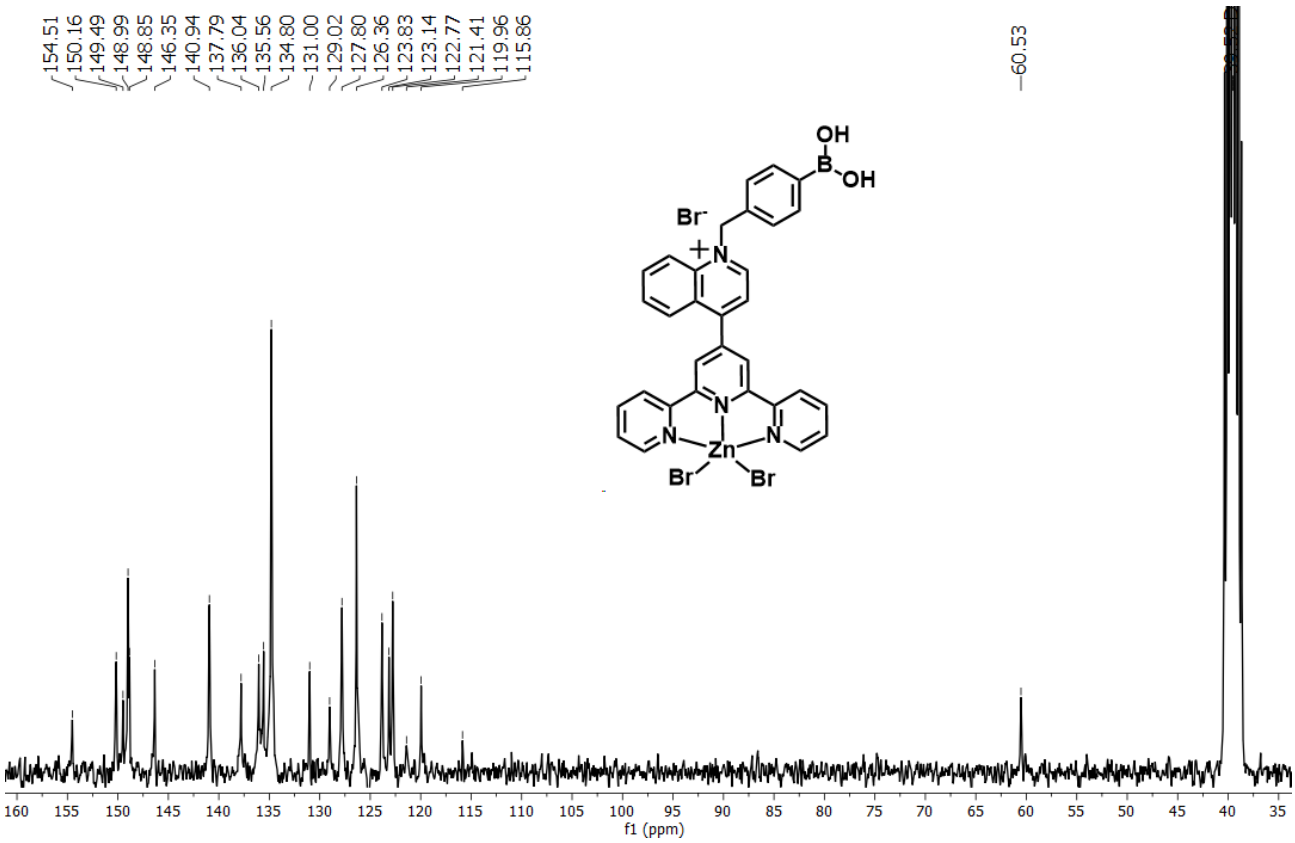

Fig. S31. ^{13}C NMR (75 MHz, 25°C) spectrum of **4Zn** in DMSO-d_6.

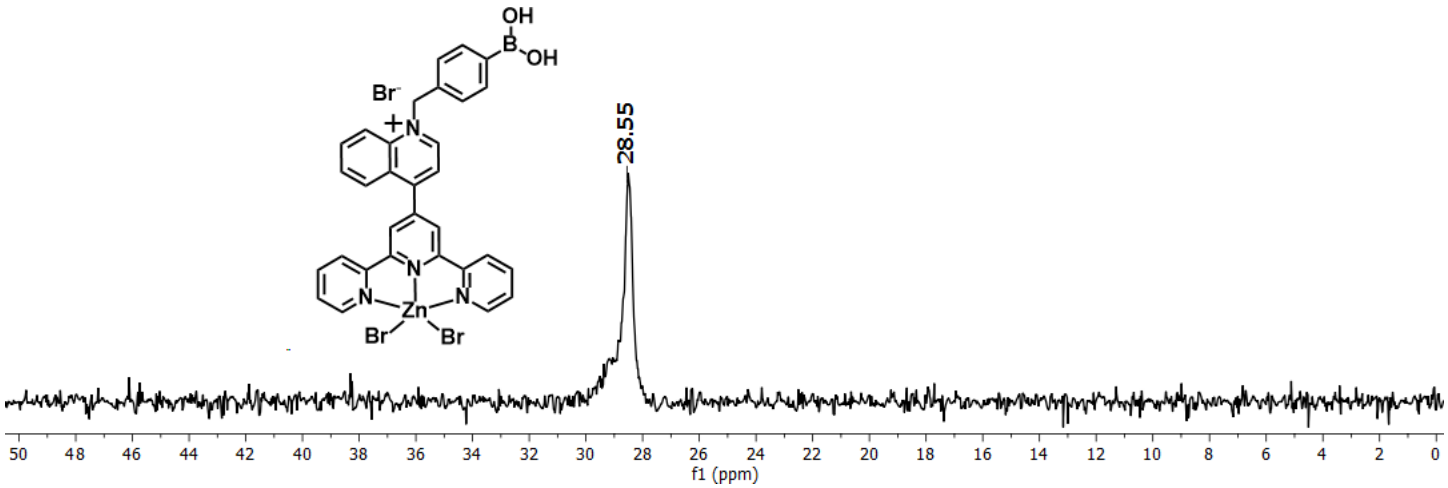

Fig. S32. ^{11}B NMR (96 MHz, 25 °C) spectrum of **4Zn** in MeOD-DMSO-d_6 (v/v, 4/1).

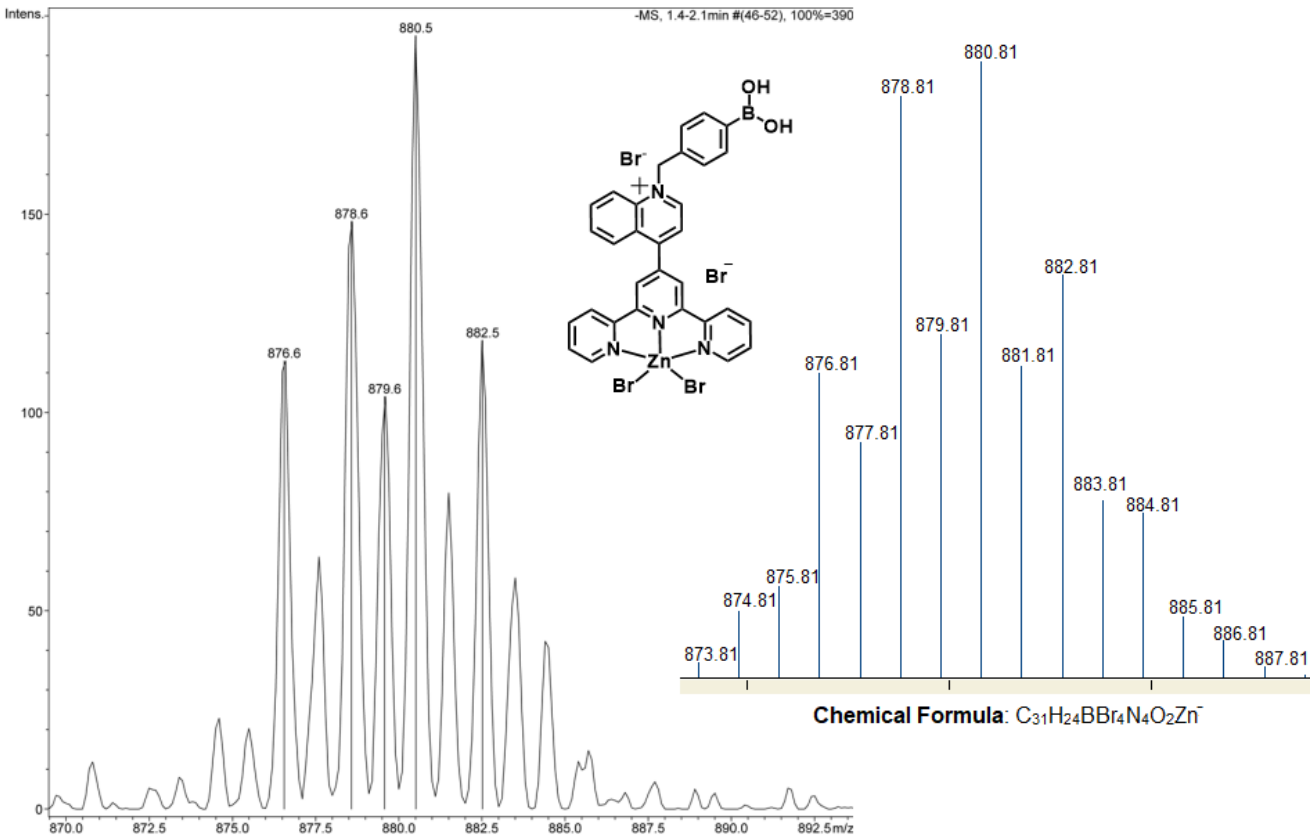

Fig. S33. Negative scan MS-ESI spectrum of **4Zn**. Inset: theoretically calculated MS isotopic patterns.

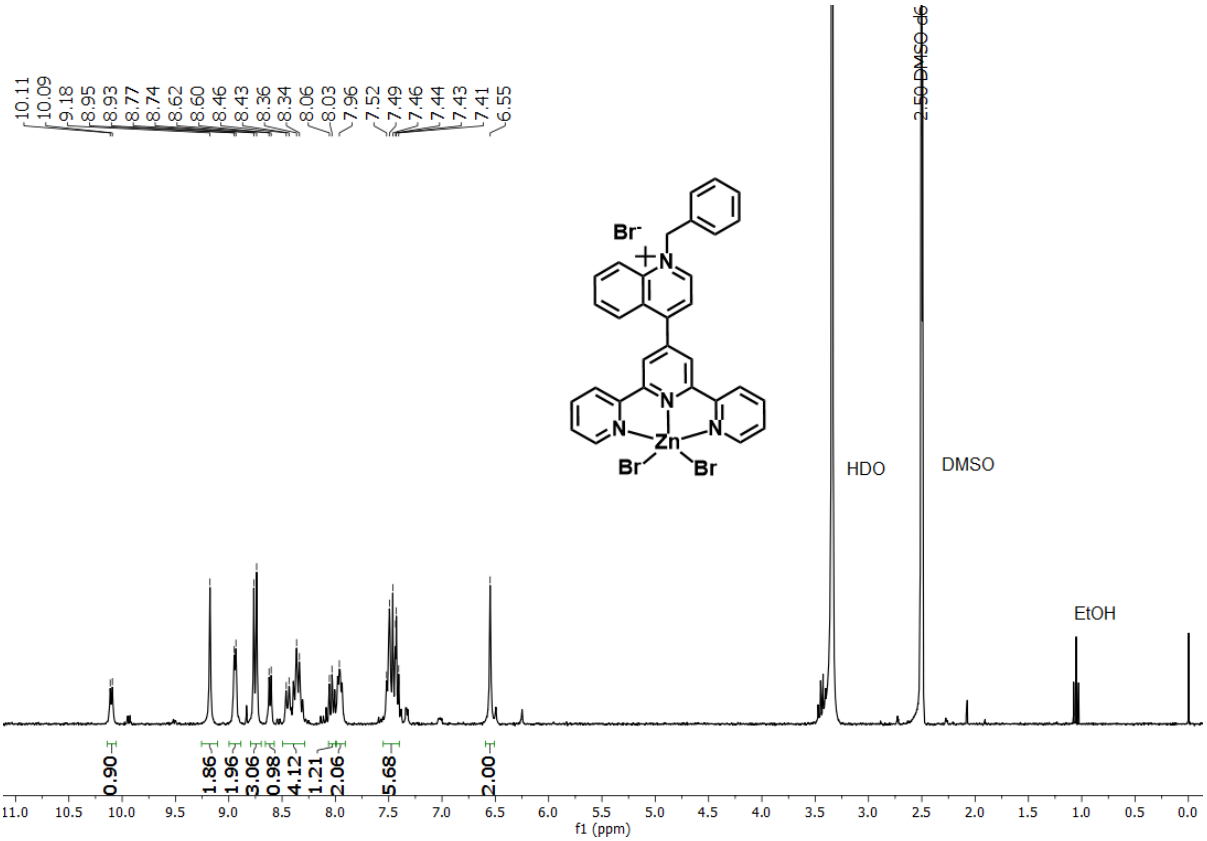

Fig. S34. ^{1}H NMR (300 MHz, 25°C) spectrum of **5Zn** in DMSO-d_6.

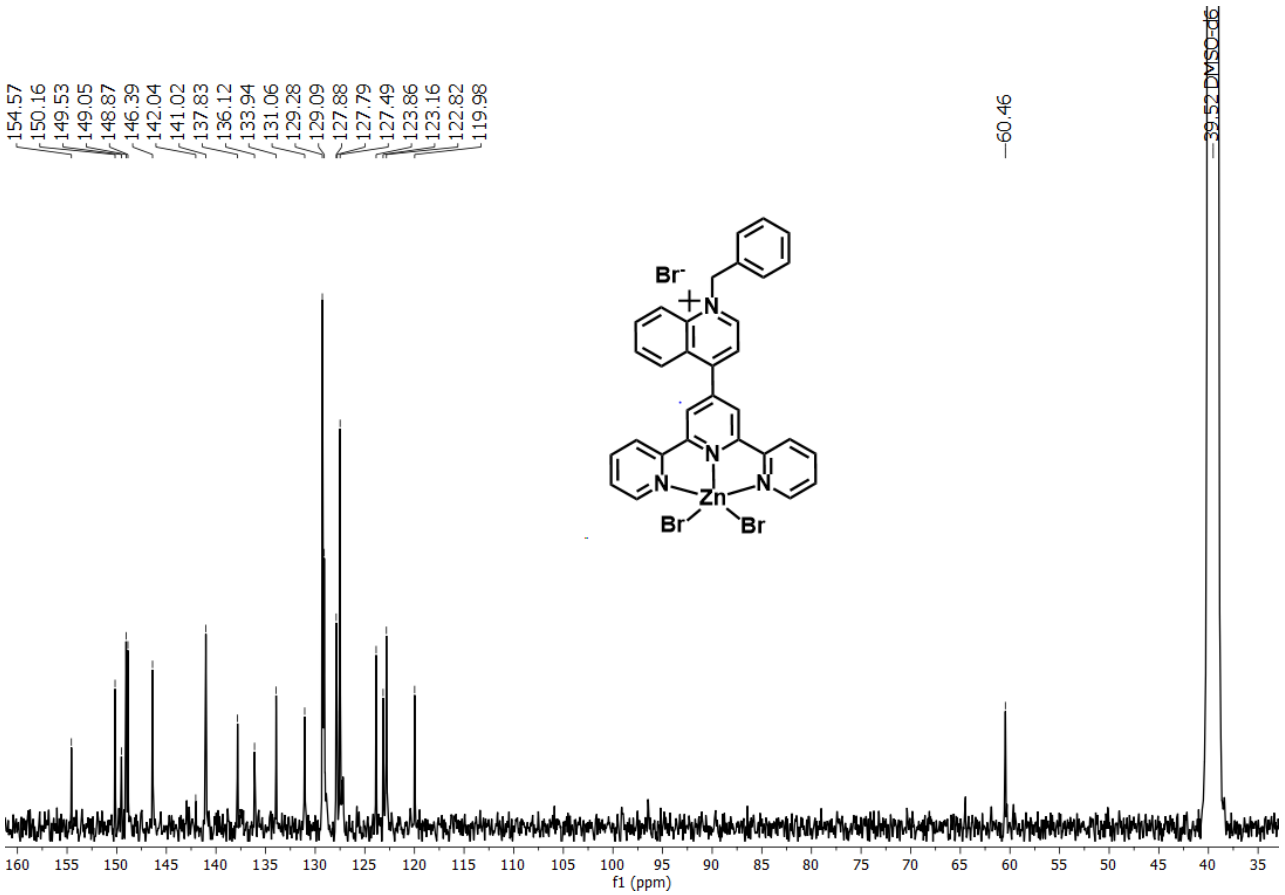

Fig. S35. ^{13}C NMR (75 MHz, 25°C) spectrum of **5Zn** in DMSO-d_6.

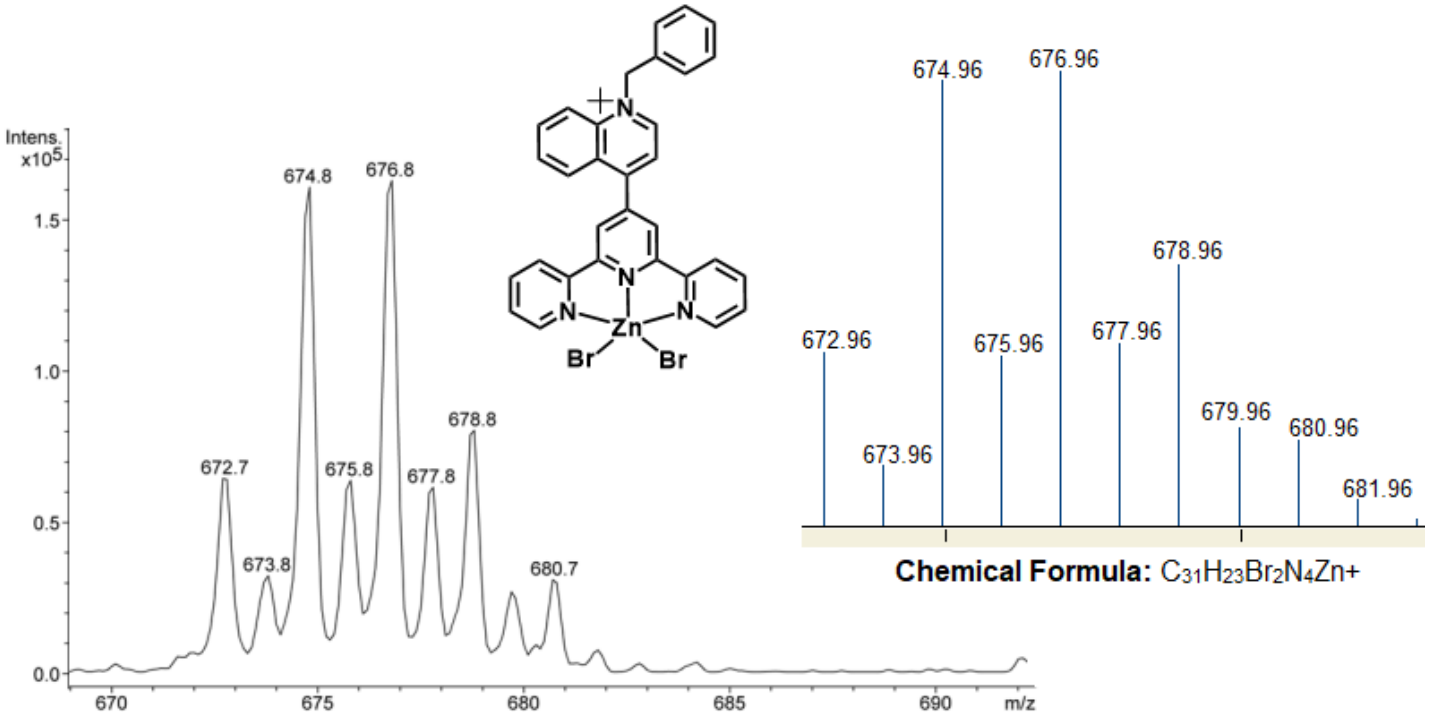

Fig. S36. Positive scan MS-ESI spectrum of **5Zn**. Inset: theoretically calculated MS isotopic patterns.

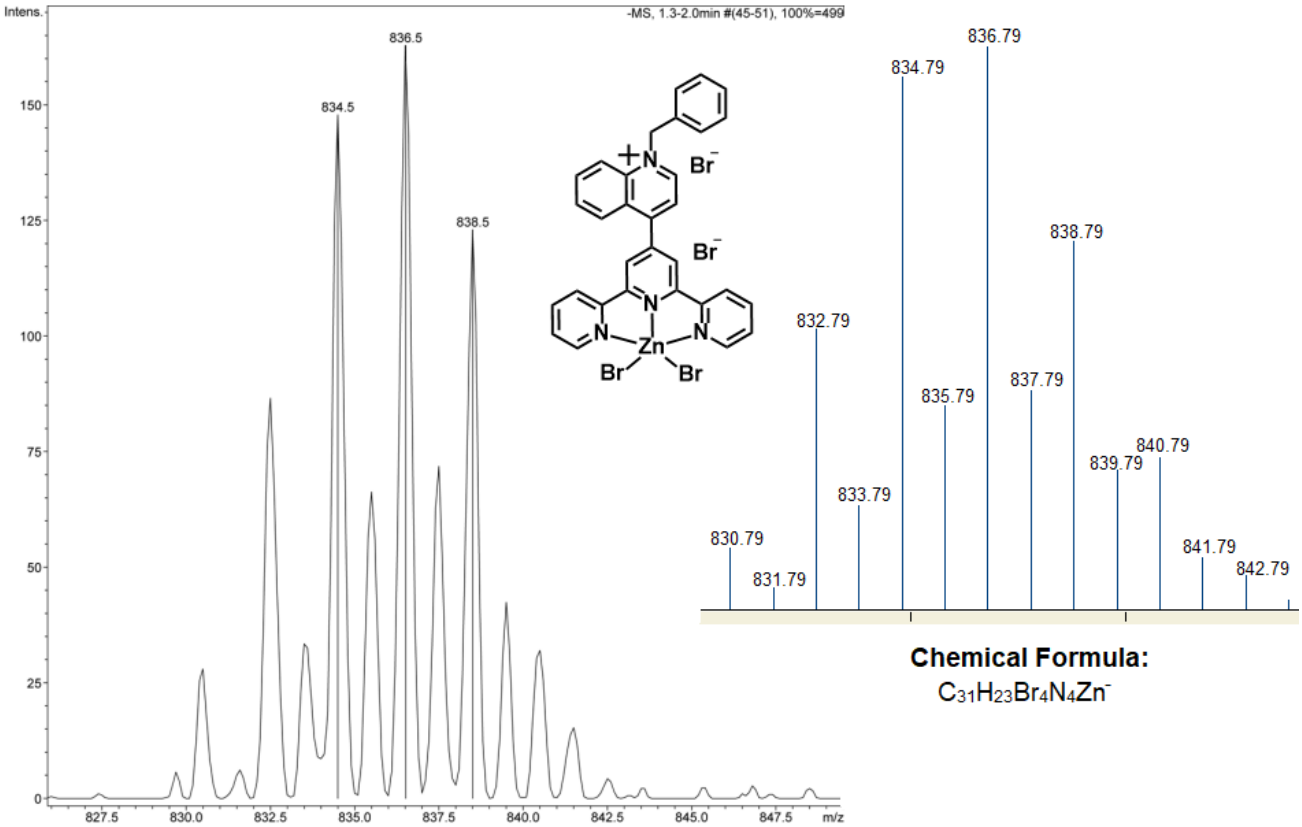

Fig. S37. Negative scan MS-ESI spectrum of **5Zn**. Inset: theoretically calculated MS isotopic patterns.

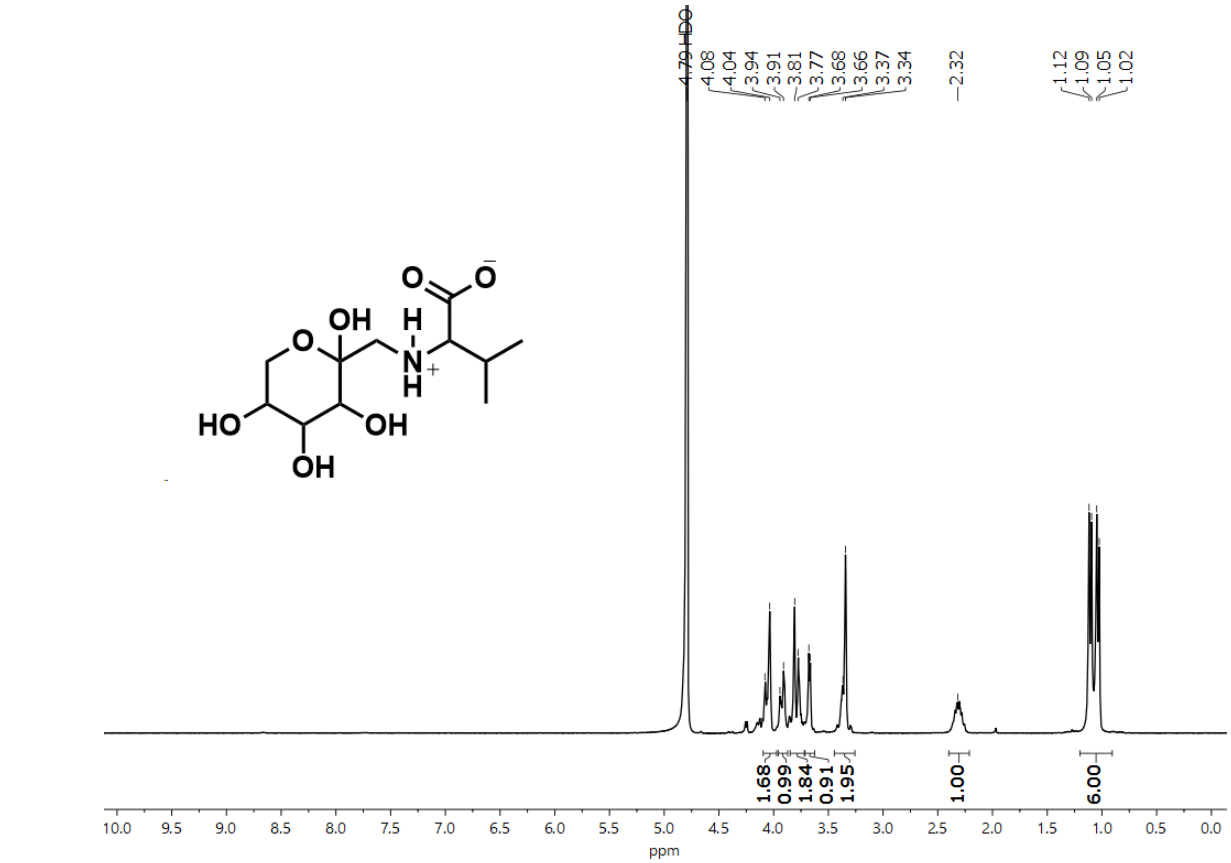

Fig. S38. ^{1}H NMR (300 MHz, 25°C) spectrum of **FV** in D_2O.

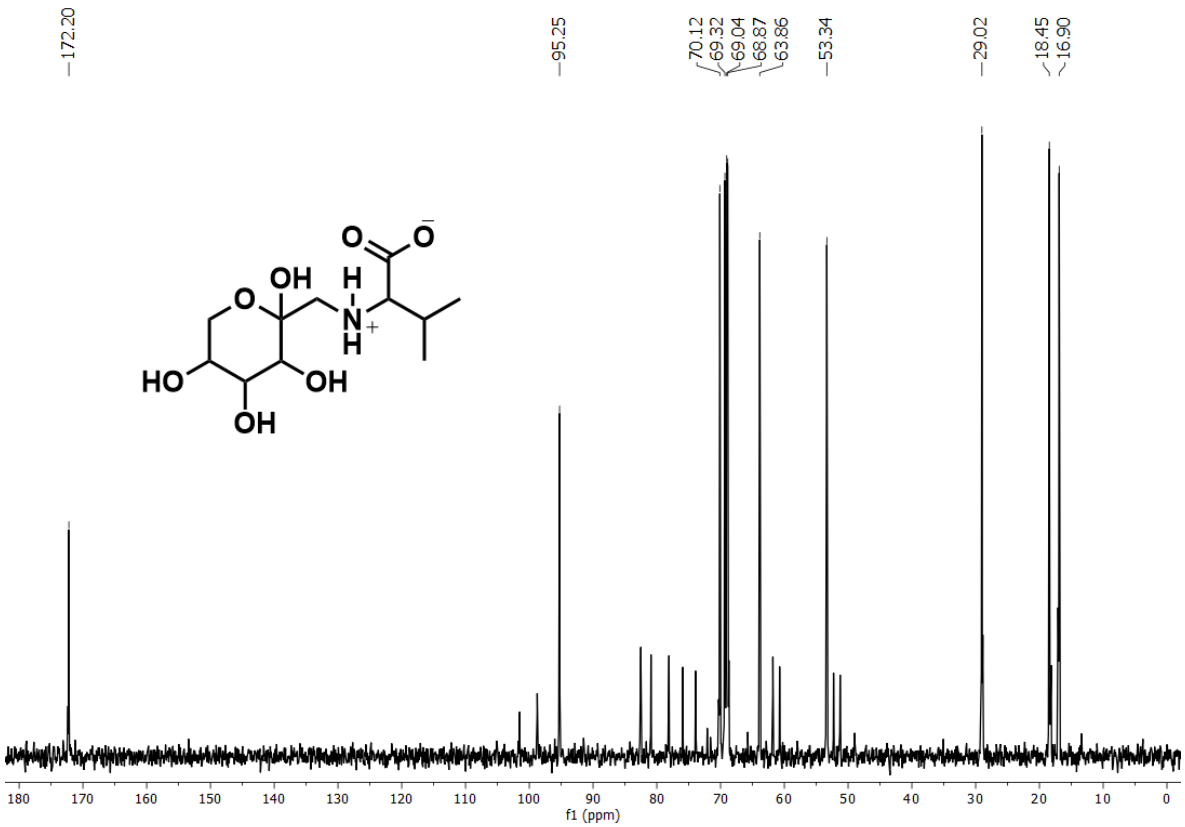

Fig. S39. ^{13}C NMR (75 MHz, 25°C) spectrum of **FV** in D_2O.

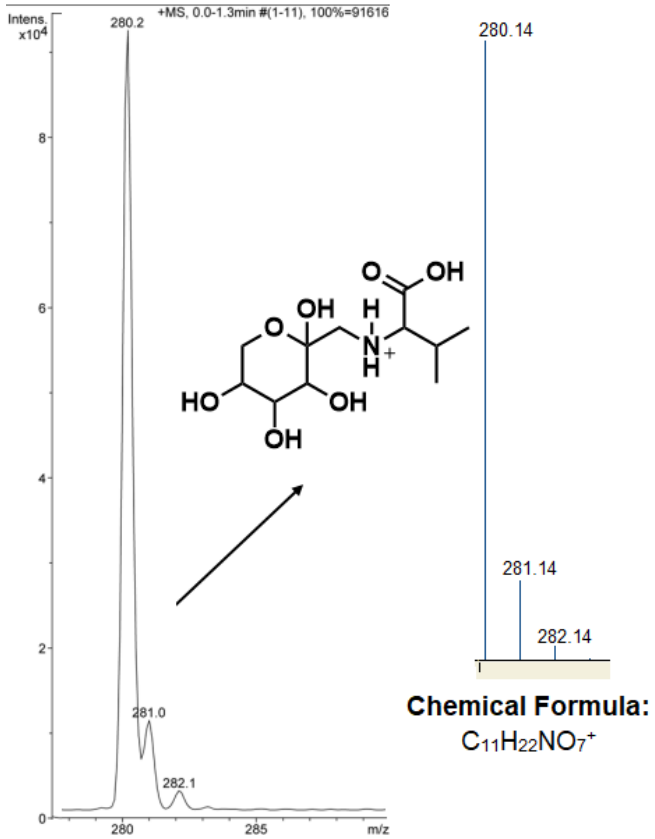

Fig. S40. Positive scan MS-ESI spectrum of **FV**. Inset: theoretically calculated MS isotopic patterns.

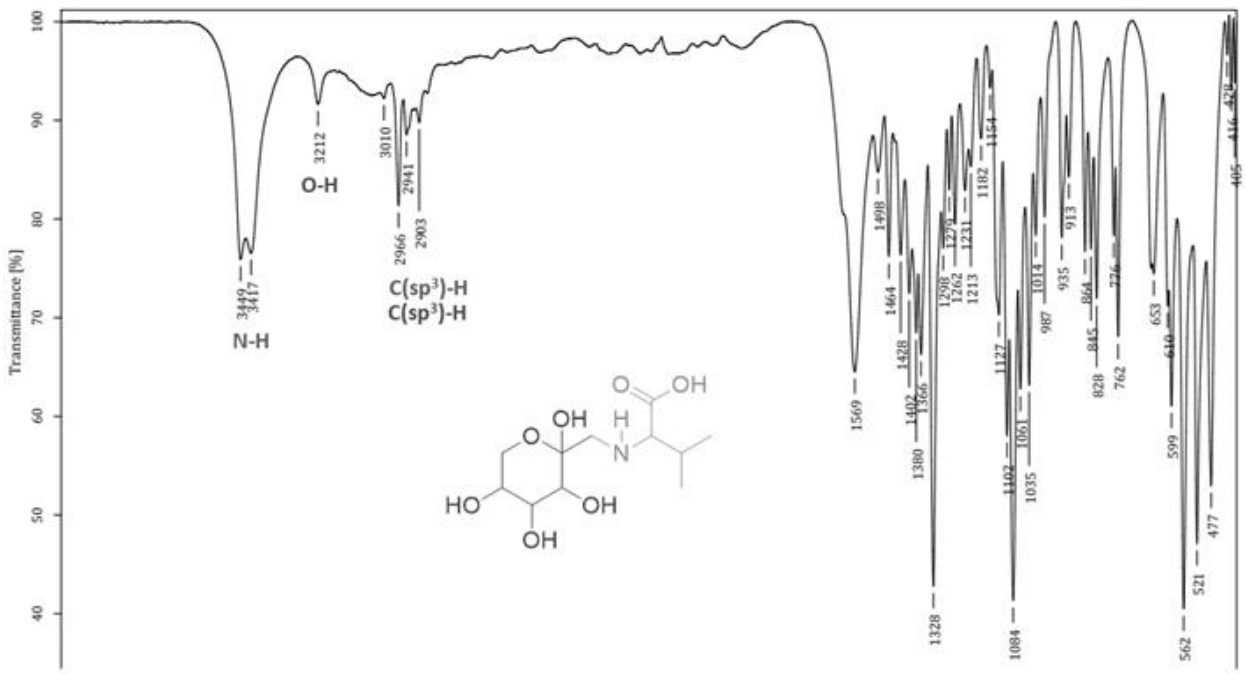

Fig. S41. IR (ATR) spectrum of **FV**.

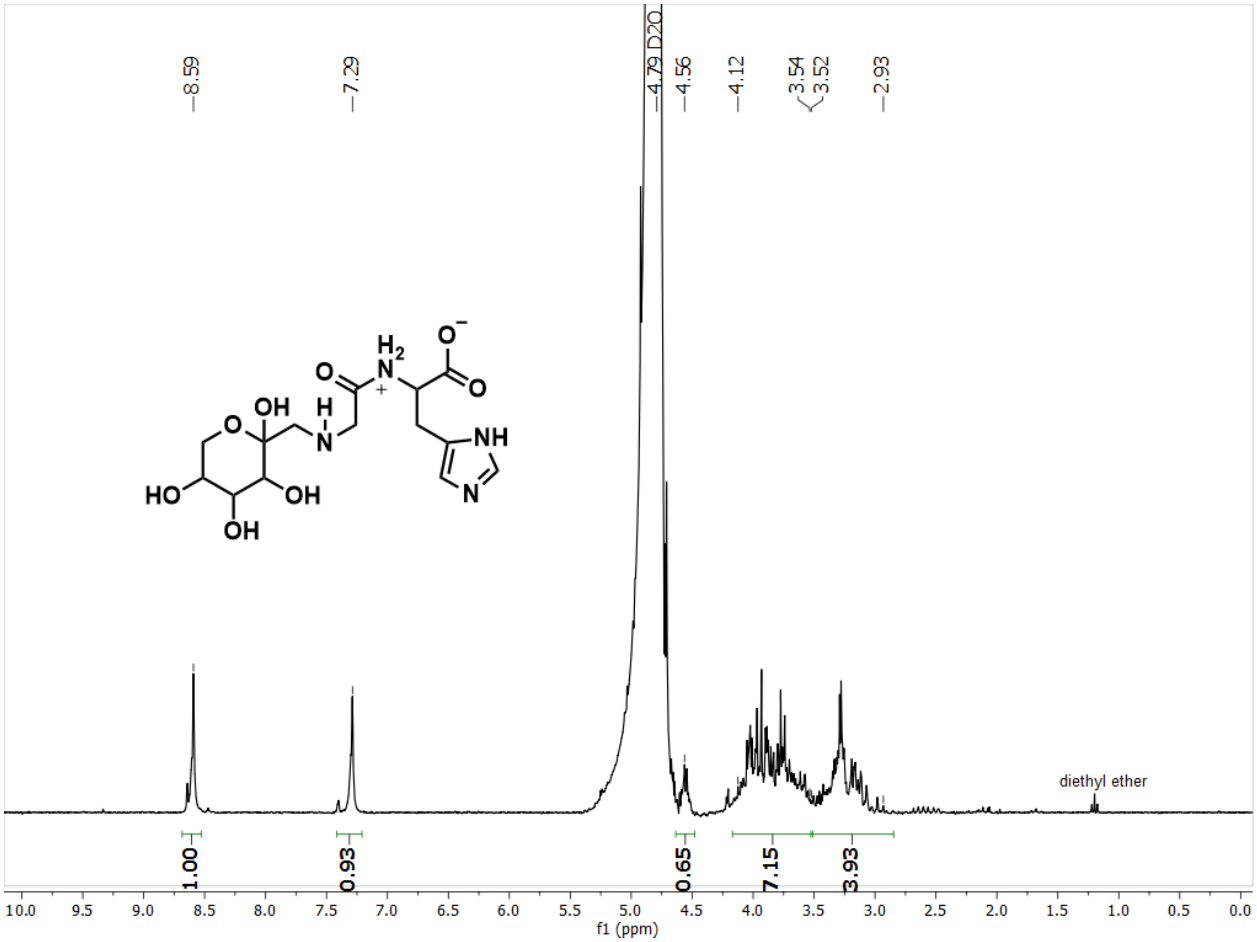

Fig. S42. ^{1}H NMR (300 MHz, 25°C) spectrum of **FGH** in D_2O.

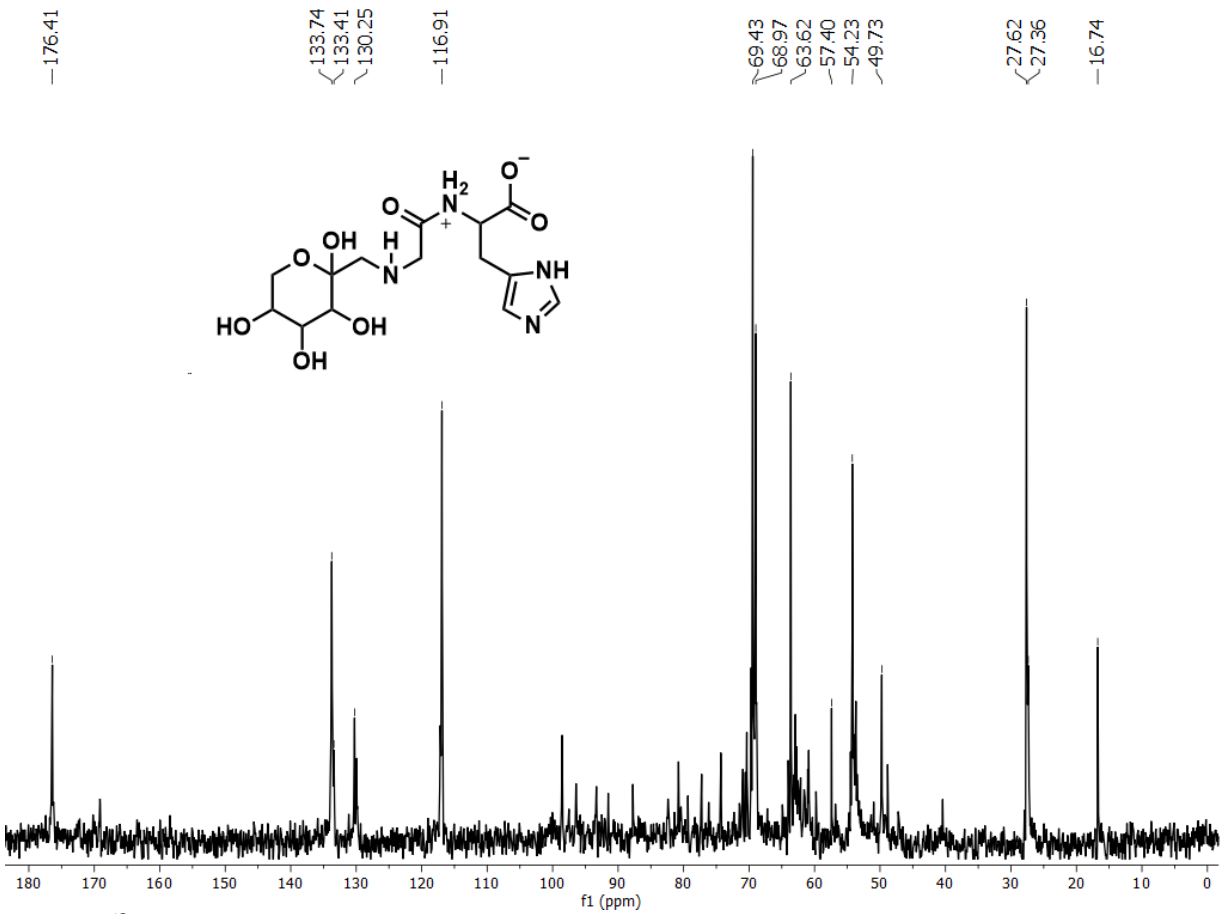

Fig. S43. ^{13}C NMR (75 MHz, 25°C) spectrum of **FGH** in D_2O.

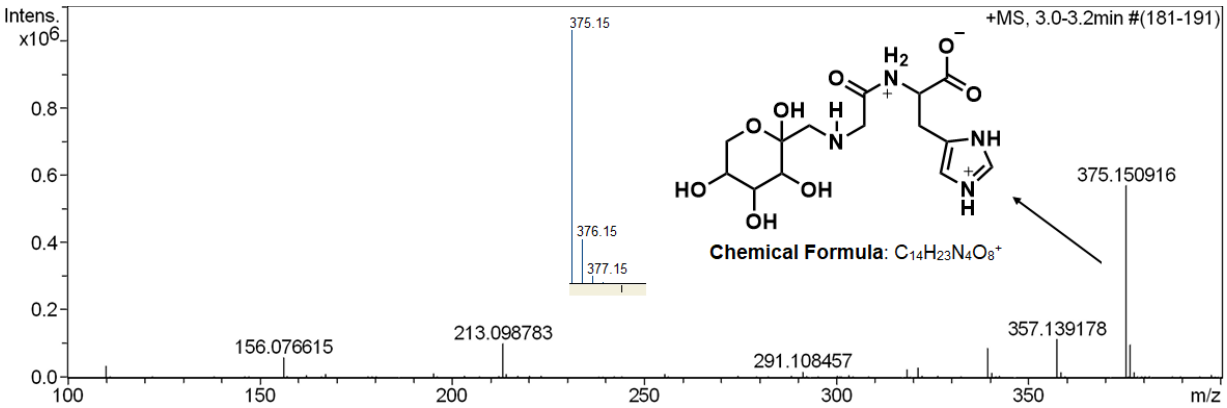

Fig. S44. High-resolution mass spectrum by a positive scan of ESI of **FGH**. Inset: theoretically calculated MS isotopic patterns.

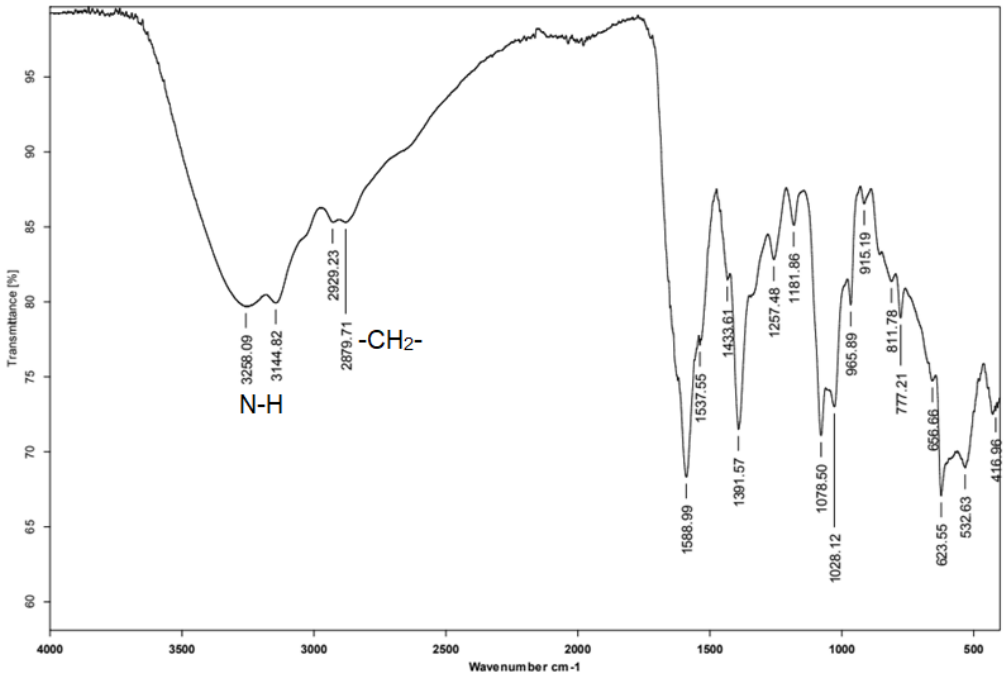

Fig. S45. IR (ATR) spectrum of **FGH**.

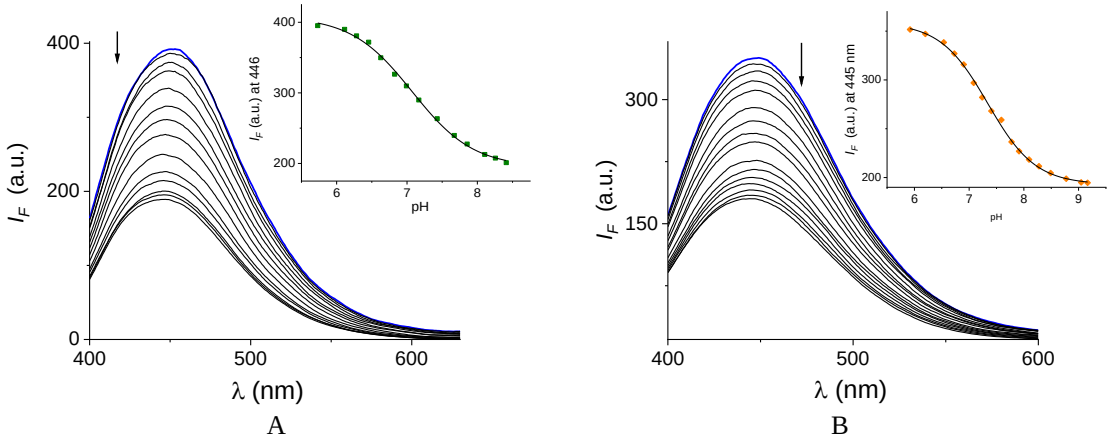

Fig. S46. Fluorescence spectra of (A) **2Zn** and (B) **3Zn** (20 μM, each one) in buffered aqueous (λ_{ex} = 330 nm) at different pH values.

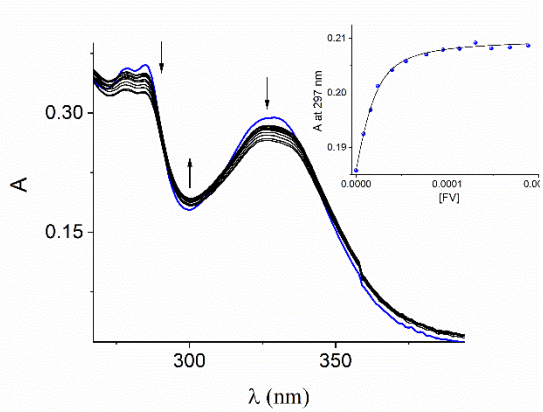

Fig. S47. UV-vis titration of aqueous solution of **3Zn** (20 μM) with FV at pH= 7.4 (10 mM, MOPS). The inset shows the profile of absorbance at 297 nm for increasing amounts of FV. The line was obtained by fitting the data to a 1:1 binding model.

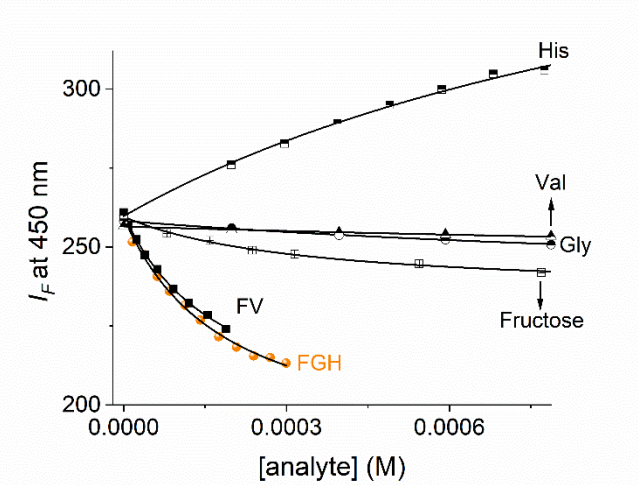

Fig. S48. Fluorimetric titration (λ_{ex}= 330 nm) of aqueous solutions of **4Zn** (20 μM) upon addition of increasing amounts of fructosyl-amino acids, His, Gly, Val and fructose at pH 7.4. The solid lines were obtained by fitting to eqn. (1).

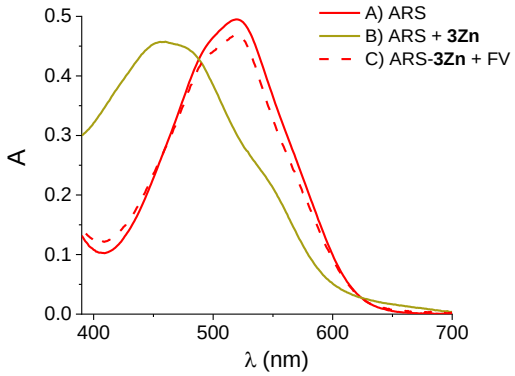

Fig. S49. (A) Absorbance of free ARS (100 μM) at pH 7.4. (B) ARS (100 μM) with **3Zn** at 110 μM. (C) ARS (100 μM) with **3Zn** at 110 mM and FV at 1.0 mM.

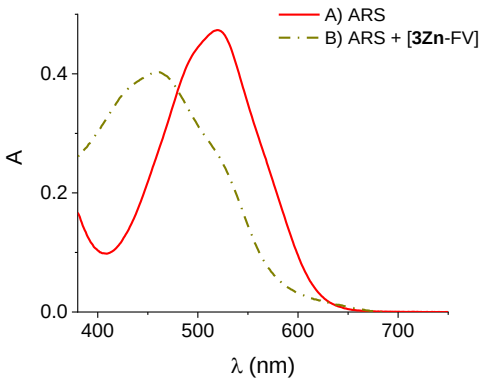

Fig. S50. (A) Absorbance of free ARS (100 μM) at pH 7.4. (B) Absorbance of ARS (100 μM) in the presence of the complex prepared in situ **3Zn**-FV (110 μM, each component) at pH= 7.4.